The Potential of Esters as Renewable Fuels: Determination of Laminar Burning Velocities

Master's Thesis

Anas Ali Bnayan

Supervisor:

Dr.Elna Heimdal Nilsson
Division of Combustion Physics
Lund University

Department of Physics

Division of Combustion Physics

Lund University

February 2013

Abstract

Biodiesel fuel is widely used as a clean fuel in car engines. Ester fuels are a one kind of a biodiesel fuel which includes many chemical compounds. Due to their chemical and physical properties these esters are difficult to investigate in a laboratory. The heat flux method was used in this study to determine adiabatic burning velocity.

The heat flux method for determination of laminar burning velocities is a useful method since the property can be determined directly, without corrections or extrapolations that apply to other burning methods.

In the present study, the burning velocity of straight chain acetate ester fuels (methyl acetate, ethyl acetate and n-propyl acetate) have been determined. The laminar burning velocities of C3-C5 esters/air were measured by liquid heat flux installation at atmospheric pressure, initial temperatures $(298 - 348\ K)$ and equivalence ratios $(0.7 - 1.5)$. The main goal of this project is to provide new experimental data and investigate laminar flame speeds as a function of carbon chain length. There is no literature date available apart from the data found in this work, so a comparison between these results is performed at different temperatures for each ester. A good resemblance can be claimed from this comparison and limited studies related to these fuels; whereas, all results curvatures have the same trends and the maximum velocity for each temperature under study found at $\varphi = 1.1$. Also, the results of esters are compared against each other and other esters found in literature at the same temperature in order to assess the effects of carbon chain length on laminar burning velocity. A good resemblance is found between ester group and alkane group with corresponding carbon chain length. Lastly, temperature dependencies with laminar flame speeds have been studied and power exponents have been determined as a function of equivalence ratio.

This research presents new experimental data for the biodiesel ester group. The adiabatic burning velocity of these esters was determined using the heat flux method. The results presented can be assumed with high level of accuracy $\pm 1\ cm/s$.

Acknowledgement

Contents

Chapter 1

Introduction

1.1 Motivation

The world, as it is today, massively relies on fossil fuels and nuclear power, in order to generate energy. This results in a system that lacks diversity and security, that threaten public health and jeopardizes the stability of Earth's climate, while robbing future generations of clean air, clean water, and energy independence. Due to these risks, renewable energy has emerged as a primary tool in the global strategic race toward a low carbon economy.

Contrarily to fossil fuels, which are the at a risk of depleting, renewable energy such as solar power, wind power and biofuel, is inexhaustible and presents clear advantages on several levels. Countries that are successful in this race will gain strong economy, while making contribution to climate policies that may arise their international political standing and reduce their dependency on imported energy [1].

Among many resources of renewable energy, international investment focuses particularly on biofuels, supporting the research on reducing the cost of squeezing fuel out of biomass, aiming to make it competitive with the fluctuating price of oil. To achieve that goal, scientists have to find efficient, elegant ways to extract molecules such as glucose — a crucial chemical from which ethanol and other products are made from lignocellulose, the hard woody part of plants, animal fat, plant residues and other kinds of crops [2].

The current work aims to contribute to the creation of new biofuels engines by investigating on the laminar burning velocity of different kind of biodiesel (Ester fuel group) using a heat flux method.

1.2 Background

 In particular this project will focus on the biodiesel fuels. Ester fuels are one kind of biodiesel fuel including many chemical compounds. Fuel mixtures of mono-alkyl esters of long chain fatty acids derived from vegetable oils and other products. Biodiesel fuel is widely used as a clean fuel in engine cars these days. Biodiesel fuels can be used alone or as a blend mixture with conventional diesel.

The ester is biofuel characterized by a chain length of roughly 16 to 18 carbon atoms. Due to their chemical and physical properties these long chained esters are difficult to investigate in a

laboratory. Therefore this study is performed on shorter chained esters like methyl formate, methyl acetate and ethyl acetate.

The laminar burning velocity is the linear velocity of the flame front normal to itself relative to unburned fuel mixture. This is a unique combustion parameter for every combustible gas mixture as it contains fundamental information of combustible fuel properties and validation of chemical kinetic mechanisms to take into account in any combustion research [3]. Experimental determinations of laminar burning velocities of esters are few.

The heat flux method for determination of laminar burning velocities is a useful method since the property can be determined directly, without corrections or extrapolations that apply to other methods. The method has recently been extended to use for liquid fuels based on [4], but has not been applied to research concerning esters.

However, the database concerning the combustion characteristics of ethyl esters and their kinetics models are relatively scarce. The following publications present experimental and kinetic studies of ester fuels related to the same esters as will be used in the present study or esters in the same alkyl group but applied in different conditions or in different combustion methods. All the previous studies mentioned in the following text are summarized in Table 1.2.

In 2009, Seshadri et al. [5] published an experimental and kinetic modelling study of the combustion of methyl decanoate (MD). MD combustion was investigated in non-premixed and non-uniform flows, using counterflow configuration for experimental data and a Skeletal mechanism for numerical results. In this study a fuel stream was made up with vaporized MD and nitrogen and oxidizer steam with air. The mass fraction of fuel in the fuel stream was measured in terms of temperature of the oxidizer stream as a function of the strain rate extinction and critical conditions of ignition. Experimental data were found to agree with computational data within acceptable accuracy.

Liu et al. [6] presented in 2011 an experimental and kinetic modelling study of the non-premixed ignition temperature of n-butanol iso-butanoal and methyl butanoate in liquid pool assembly by heated oxidizer in a stagnation flow for system pressure of 1 and 3 atm. In addition, the stretch-corrected laminar flame speeds of mixtures of air and n-butanol/iso-butanol/methyl butanoate determined using constant pressure spherical bomb method at atmospheric pressure up to 2 atm, for an extensive range of equivalence ratios (0.7-1.7). The laminar flame speed for these fuels were measured at an initial temperature of pre-mixed gas $353\ K$. The results are experimental values of laminar flame speeds of methyl butanoate at both pressures less than simulated values.

In the same year Dooley et al. [7] studied the oxidation of methyl formate, the simplest methyl ester, in three experimental environments over a variable range of combustion conditions. In this study laminar burning velocities of outwardly propagating spherical CH_3OCH/air were determined for stoichiometries ranging from $(0.8 - 1.6)$ at atmospheric pressure using a

pressure-released-type high-pressure chamber. Experimental results were compared with numerical calculations. The measured laminar burning velocity of methyl formate/air mixtures were shown to be consistent with that of other hydrocarbons and oxygenates with peak burning velocity observed at value of $\varphi = 1.2$.
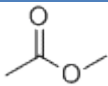
Wang et al. [8] in 2011 published a study of C4 and C10 methyl ester flames (methyl butanoate, methyl crotonate and methyl decanoate) in laminar premixed and non-premixed flames. The experiments were conducted in the counter flow configuration at atmospheric pressure, for a wide range of equivalence ratios, and elevated reactant temperature $(T = 403\ K)$. They compared the experimental data against those derived for flames of n-alkanes of the similar carbon number, in order to assess the effects of saturation, the length of carbon-chain and the presence of the the ester group. The combustion results showed that the flames of methyl butanoate/air and methyl crotonate/air have a slightly higher laminar flame speed and extinction strain rates. Also, the results explained that the presence of the ester group has a retarding effect on the overall mixture reactivity and diminishes as the carbon chain increase.

In 2012, Dayma et al. [9] studied the ignition of $C4 - C7$ ethyl ester (ethyl acetate EA, ethyl propionate EP and ethyl butanoate EB) to measure pre-mixed ethyl ester/air laminar flames in the spherical combustion chamber over a range of pressure $(1 - 10\ bar)$, initial temperatures $(323 - 473\ K)$ and equivalence ratios $(0.7 - 1.5)$. In the same study kinetic modelling of oxidation of EA, EP and EB in the same conditions as mentioned before were compared with experimental results. The results had good agreement between measured values and kinetic modelling results.

The aim of this project is two fold: the first goal provides new experimental results for combustion of five ethyl esters (see Table 1.1) by measuring burning velocities of pre-mixed laminar flames over a range of equivalence ratios and different temperatures using the heat flux method, and compare these results with limited available literature gathered in Table 1.2. The second goal of this study investigates propagation burning velocity with increasing carbon chain from C3 - C7.

The following table shows some chemical properties for esters under study in this work.

Table1.1: List of chemical properties of esters used in this study [10]

Easter Name	Chemical Formula	Chemical Name	Boiling point	Density	Molar mass MW	Risk statements
Methyl acetate	C3H6O2		57-58 °C(lit.)	0.932 g/ml at 25 °C(lit.)	74.08 g/mole	Highly Flammable, Irritant, repeated exposure may cause skin dryness or cracking.
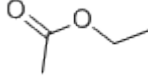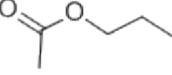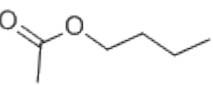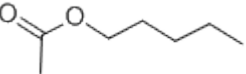
Ethyl acetate	C4H8O2		76.5-77.5 °C(lit.)	0.902 g/ml at 25 °C(lit.)	88.11 g/mole	Highly Flammable, Irritant, Harmful, Toxic
n-Propyl acetate	C5H10O2		102-103 °C(lit.)	0.888 g/ml at 25 °C(lit.)	102.13 g/mole	Highly Flammable, Harmful, Irritant, Vapors may cause drowsiness and dizziness.
n-Butyl acetate	C6H12O2		124-126 °C(lit.)	0.88 g/ml at 25 °C(lit.)	116.16 g/mole	Flammable Repeated exposure may cause skin dryness or cracking, Vapors may cause drowsiness and dizziness
n-Amyl acetate	C7H14O2		142-149 °C(lit.)	0.876 g/ml at 25 °C(lit.)	130.18 g/mole	Highly flammable, Irritant.

Table 1.2: Experimental data of ester fuel with different combustion method in variable conditions

Ester name	Burning method	Temperature (K)	Pressure	Equivalence Ratio (φ)	Reference
Ethyl,(Acetate, Propanouate& Butanoate)	Spherical combustion bomb	(323 – 473)	(1-10) bar	(0.7 – 1.5)	Dayma et al.
Methyl Formate	Dual-chamber cylindrical bomb	295±2	1 atm	(0.8 – 1.6)	Dooley et al.
Methyl Butanoate & Crotonate	Counterflow configuration	403	1 atm	(0.7 – 1.5)	Wang et al.
n-butanol,iso-butanol & Methyl butanoate	Spherical combustion chamber	353	(1–2) atm	(0.7 – 1.7)	Liu et al.
Methyl decanoate	Counterflow configuration	478	1 atm	---	Seshadri et al.

1.3 Report Overview

The heat flux method is used in this experiment to measure laminar burning velocities for ester fuels based on Lizpig et al. [4] study of liquid fuel. In chapter 1 motivation to study these esters group (Table 1.1) using a heat flux method is discussed and related literature review is mentioned, also general chemical properties was tabulated. Chapter 2 the principle of the heat flux method and experimental setup is briefly discussed, also laminar flame calculation and partial pressure limitation are discussed. In the same chapter probable error sources in this experiment are mentioned. In chapter 3 mass flow controller calibration is elucidated in details to obtain accurate flow measurements. Chapter 4 measurement data for various esters with different temperatures $(298\,K - 348\,K)$ and equivalence ratios are presented and discussed, where a comparison is made with limited literature data. In last chapter general conclusions are made and recommendations are given.

Chapter 2

Heat Flux Method

2.1 Introduction

Historically, the heat flux method started from the Botha and Spalding [11] work. They used a porous plug burner to determine the heat loss for stabilizing the flame by measuring the temperature variation of the water used for cooling the burner. In reality this mechanism was not active, since the temperature increase of the cooling water is too small. Also the adiabatic velocity was determined by extrapolation to zero heat loss. De Goey at al. [12] proposed the heat flux method to stabilize an adiabatic premixed laminar flame on a flat flame burner. In 1993, Van Maaren [13] introduced the concept of perforated plate burner to stabilize the flame by using a brass plate of 2mm thickness. Also, the perforated pattern with hexagonal small holes was used to ensure the stabilize flame remains flat. In this design thermocouples were attached in different radial position on the burner plate to measure the temperature distribution corresponding to heat loss from the flame to the burner. The second improvement of the heat flux method was made by Botha and Spalding. The burner plate was heated and fixed at temperature around 85 ℃. This improvement gives very accurate burning velocity measurements because the heat loss of stabilizing the flame can be compensated by the heat gain of the unburnt gas mixture.

Van Maaren [13] designed a heat flux setup to measure the adiabatic laminar flame speed of gaseous fuel. However, Meuwissen [14] extended the use of the heat flux setup by using an evaporator to mix liquid with oxidizer to find the burning velocity of liquid fuel. After that van Lipzig [15] used an almost identical setup for liquid fuel designed by Meuwissen. The new setup had some improvements constructed and a new Labview program was designed. In the current work the same setup of van Lipzig will be used to measure laminar burning velocity of new bio-diesel fuels.

2.2 Fundamental Principle

The heat flux method is a recent technique to measure laminar burning velocity. This method is based on tuning velocity of the unburnt gas mixture to a value satisfying the adiabatic condition of zero heat losses. The basic principle depends on the heat gain by an unburnt gas mixture from the burner plate equal heat loss from the flame to the burner plate, which is necessary to stabilize the flame. At adiabatic burning velocity condition zero heat flux is obtained. A detailed description of the heat flux method is found elsewhere [14, 16]. The net heat flux or the difference between heat loss and heat gain is responsible for the temperature distribution on the burner plate measured by thermocouples distributed in the different radial placements. The adiabatic flame velocity can be found at constant temperature profile across the burner plate and therefore zero heat flux will be obtained. The temperature profile depends on the burner plate temperature readings by thermocouples (T_p) in the axial direction. Because the thickness of the burner plate is very small compared to the plate radius, the temperature distribution only depends on the radius. By comparing the temperature profile on the burner plate with free flame, the same behaviour will be turned in stabilizing an adiabatic flame. Figure (2.1) shows both flame trends schematically.
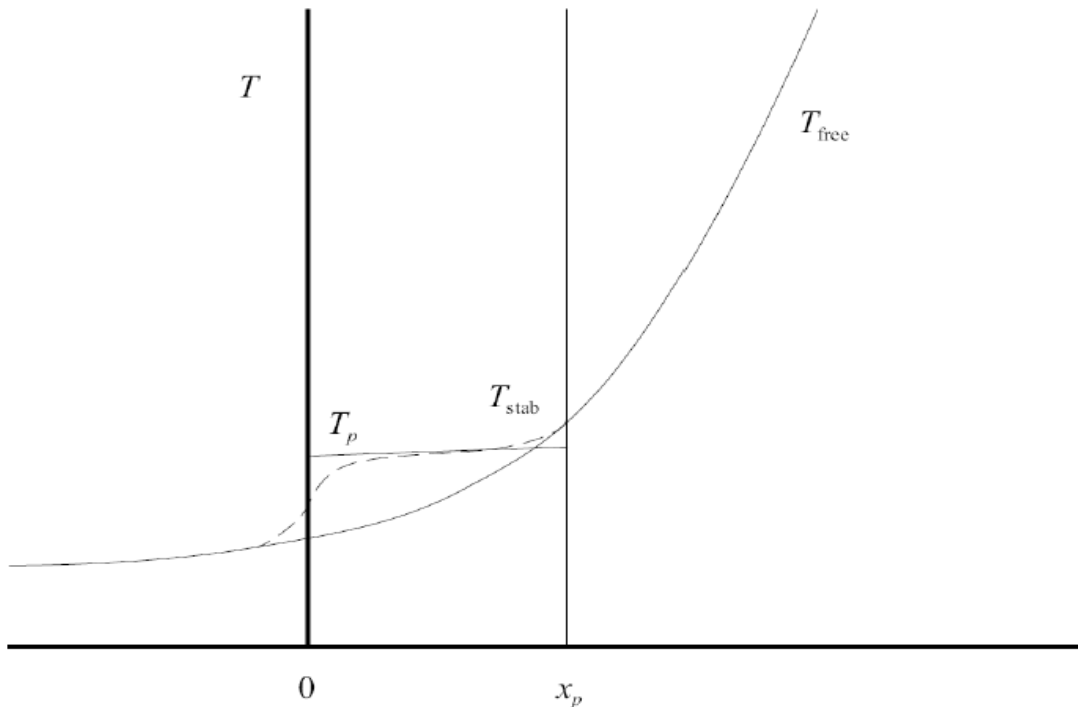

Figure 2.1: The temperature profile of a free flame (line, T_{free}) compared to the temperature profile of a flame stabilized on the burner plate (dashed,T_{stable}). T_p indicates the temperature of the burner plate, from [14].

This proofs that the heat exchange is only affected around the burner plate. The temperature profile of the burner plate is given by the following equation (2.1).

$$\overline{T_p} = T_{Centre} + \frac{q}{4\lambda_p h} r^2 \ \text{.....................................} \ \text{Eq. (2.1)}$$

where, $\overline{T_p}$ is the mean temperature of the burner plate over the burner thickness at radial position r. T_{Center} is the thickness averaged temperature of the burner plate at the centre ($r = 0$). h is the burner plate thickness and the λ_p is the heat conductivity coefficient of the plate. The main parameter q is the net heat flux (the difference between heat flux from the flame to burner plate and the heat flux from the plate to the unburned mixture).

It is convenient to write the last equation (2.2) to the following formula for practical uses:

$$\overline{T_p} = T_{Cenetr} + \alpha^2 r^2 \ \text{.............................} \ \text{Eq. (2.2)}$$

$$\text{Where, } \alpha^2 = -\frac{q}{4\lambda_p h} \ \text{.............................} \ \text{Eq. (2.3)}$$

It is obvious by looking for an equation (2.2) that the temperature profile in the burner plate has a parabolic shape with its peak at the centre of the perforated plate. The temperature profile can be approximated by a second order polynomial using the mean temperatures measured by thermocouples to determine the α^2 value for each gas velocity.

The laminar flame speed at adiabatic condition is determined from interpolation by setting different unburnt gas velocities for each equivalence ratio and certain temperature. The parabolic coefficient α^2 will be calculated for each velocity; this coefficient take a positive value if the gas velocity (v_g) is higher than the adiabatic burning velocity (S_L) and it will be a negative value at $v_g < S_L$. A flat temperature profile occurs when the parabolic coefficient, (α^2) of the fit temperatures equal zero. Now to find adiabatic burning velocity (S_L), a flat temperature profile with $\alpha^2 = 0$ should be achieved. A virtual example of determining the adiabatic burning velocity can be explained by using a Figure (2.2).
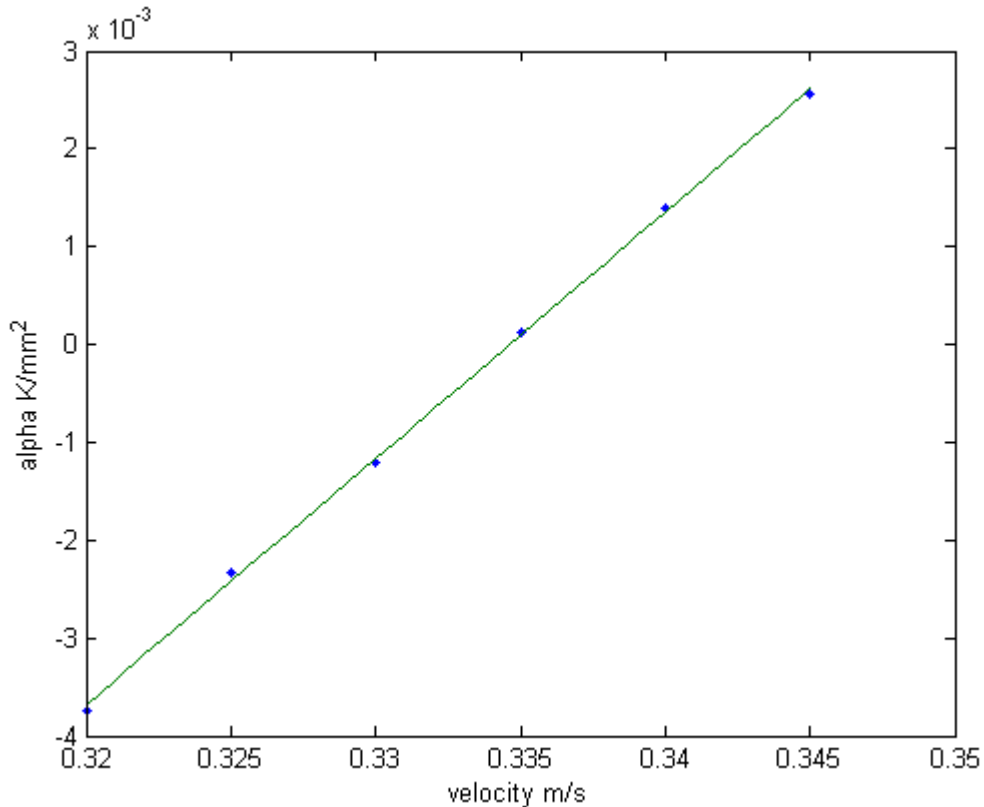
Figure 2.2: Parabolic coefficient as a function of gas velocity at plenum chamber temperature $T = 308\,K$ and $\varphi = 1.0$

The figure shows a linear relation between the velocities of the unburned gas mixture and parabolic coefficient near the adiabatic burning velocity. The adiabatic burning velocity is found by applying a linear interpolation of this fit at parabolic coefficient $\alpha^2 = 0$. In this example the adiabatic burning velocity of Ethyl acetate is equal (33.46 cm/s) at $\varphi = 1.0$ and the temperature of unburned gas mixture is equal $T = 308\,K$.

2.3 Temperature Dependence

The laminar burning velocity depends on the unburnt gas mixture temperature and pressure of esters/air flame. The temperature dependence is determined for several equivalence ratios in the temperature range 298 K to 348 K in this study. This temperature range is restricted to the limited values by the heat flux design. The water bath is used in the current setup. The theoretical boiling point is 100 ℃; in fact a burner plate is fixed at 95 ℃ and a lower temperature can be assumed due to losses in water pipelines. As the principle of the heat flux method the unburnt gas mixture in plenum chamber is kept at a temperature difference lower than the hot water jacket of the burner plate as it will be discussed in the following section (2.6) to obtain reasonable flame structure. The laminar flame speed propagation is a function of pressure and

14

temperature of the unburnt gas mixture as mentioned before. This dependence can be represented by a simple power law relation:

$$S_L = S_{L,0} \left(\frac{T_u}{T_0}\right)^{\alpha_T} \left(\frac{P_u}{P_0}\right)^{\beta_P} \ldots\ldots\ldots\ldots\ldots\ldots\ldots\ldots\ldots\ldots\ldots\ldots\ldots \text{eq. (2.4)}$$

where the T and P are the gas mixture temperature and pressure, respectively. The subscript u denote the unburnt gas conditions and the subscript 0 refers to the reference conditions ($T = 298\ K$ and $P = 1$ atm). $S_{L,0}$ is the unstretched adiabatic burning velocity at the reference conditions. The parameters α_T and β_P depend on φ, can be determined by fitting experimental data. In the current study, the temperature dependence is only studied experimentally meaning that the temperature factor remaining in equation 2.4 the pressure factor is unity. Rewrite the the last equation 2.4 including a temperature dependence only:

$$S_L = S_{L,0} \left(\frac{T_u}{T_0}\right)^{\alpha_T} \ldots\ldots\ldots\ldots\ldots\ldots\ldots\ldots\ldots\ldots\ldots \text{Eq. (2.5)}$$

Equation (2.5) can be simplified by dividing the laminar burning velocity over unstretched adiabatic burning velocity to obtain non-dimensional burning velocity as well as non-dimensional temperature.

$$S_L \sim T_u^{\alpha_T} \ldots\ldots\ldots\ldots\ldots\ldots\ldots\ldots\ldots\ldots\ldots \text{Eq. (2.6)}$$

The linear relation between burning velocity and temperature on a log-log scale is obtained. The power exponent is determined by measuring the slope of each line at various equivalence ratios. The temperature correlation with burning velocity for all esters used in this project will be presented in Chapter 4 section (4.4) and power exponent coefficients are depicted after that for corresponding esters.

2.4 Laminar Flow Calculations

At the beginning, the adiabatic burning velocity calculation is discussed to understand the gases flow principle. A certain amount of liquid fuel and oxidant gas (air in this project) are mixed together in mixing panel to get a required mixture composition, as is further explained in section 2.4. In any combustion reaction the balanced equation has to be written and checked. In the current work the following chemical compounds will be used:

$2C_3H_6O_2 + 7O_2 \longrightarrow 6CO_2 + 6H_2O \quad \ldots\ldots\ldots\ldots\ldots\ldots\ldots\ldots\ldots \text{Eq. (2.7)}$

$C_4H_8O_2 + 5O_2 \longrightarrow 4CO_2 + 4H_2O \quad \ldots\ldots\ldots\ldots\ldots\ldots\ldots\ldots\ldots \text{Eq. (2.8)}$

$2C_5H_{12}O_2 + 13O_2 \longrightarrow 10CO_2 + 10H_2O \quad \ldots\ldots\ldots\ldots\ldots\ldots\ldots\ldots\ldots\ldots\ldots \text{Eq. (2.9)}$
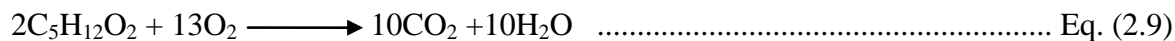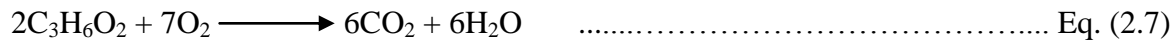
From the balance equation a molar stoichiometry factor is defined as the ratio between oxygen moles and fuel moles in the reaction. The mole stoichiometry factor in previous balance equations for esters fuel is given as follows:

$$S_{molar,C3H6O2} = \frac{7}{2} \quad\text{..} \text{Eq. (2.10)}$$

$$S_{molar,C4H8O2} = \frac{5}{1} = 5 \quad\text{..} \text{Eq. (2.11)}$$

$$S_{molar,C5H12O2} = \frac{13}{2} \quad\text{..} \text{Eq. (2.12)}$$

For stoichiometry calculations molar fractions are converted to mass fractions using the following formula:

$$S_{mass,fuel} = S_{molar} \times \frac{molecular\ weight\ of\ oxygen}{molecular\ weight\ of\ fuel} \quad\text{......} \text{Eq. (2.13)}$$

In general, the equivalence ratio is defined for the mass flow controllers in equation (2.8) and used in fluid flow calculations:

$$\varphi = S_{mas,fuel} \times \frac{m_{fuel}}{m_{oxygen}} \quad\text{.......................................} \text{Eq. (2.14)}$$

where, φ is the equivalence ratio and m is the mass for each of fuel and oxygen. Equivalence ratios can be divided into three classes: stoichiometric case ($\varphi = 1$) enough amount of oxygen present to combust all fuel exactly. Rich mixture ($\varphi > 1$) the amount of fuel in the mixture is exceeding the present air to combust it completely. Lean mixture ($\varphi < 1$) more air is present in the mixture than needed to combust the fuel.

The unburned mixture velocity is delivered by mass flow controllers, as described later, by using equivalence ratio equations and combine it with the ideal gas law. The gas velocity will be defined as:

$$v_g = \frac{R_0 T_u}{PA} \left(\frac{q_{air}}{M_{air}} + \frac{q_{fuel}}{M_{fuel}}\right) \quad\text{..} \text{Eq. (2.15)}$$

In this equation T_u is the temperature of unburned gas mixture. v_g is the desired unburned mixture velocity, R_0 the universal gas constant, M the molar mass of each air and fuel, A is the cross sectional area of the perforated burner plate, P is the actual atmospheric pressure of each measurement taken from [17] and q is a mass flow for each of air and fuel.

2.5 Partial Pressure Limitations

For investigating adiabatic burning velocity of liquid fuels, the fuel is changed into gas phase using a control evaporator mixer (CEM) and mix it with gas carrier (air). Actually this technique faces some difficulties especially if the unburned mixture is cooled down to room temperature, concerning mixtures with high equivalence ratio, high partial pressure of the fuels and high fuel molecular mass. To circumvent this problem maximum equivalence ratio of a mixture using partial pressure of fuel is calculated at room temperature, because fuel line and burner chamber operate at this temperature to get reliable results. Partial pressure (P_{fuel}) of fuel is obtained from material safety data sheet for each ester and mole fraction of the fuel can be calculated by using equation (2.16):

$$Mf_{fuel} = \frac{P_{fuel}}{P_{total}} \quad\text{...............................} \quad \text{Eq. (2.16)}$$

where, P_{total} is the total pressure of the mixture in standard atmospheric pressure. The maximum equivalence ratio can be calculated with the equation (2.17) using fuel mole fractions and molar stoichiometric ratios taken from equations (2.7) - (2.9).

$$\varphi_{max} = S_{molr} \frac{Mf_{fuel}}{Mf_{O2}(1-Mf_{fuel})} \quad\text{..........................} \quad \text{Eq. (2.17)}$$

where, Mf_{O2} is the mole fraction of oxygen present in the air [18]. The maximum equivalence ratio of room temperature is calculated at each ester fuel and present in table (2.1).

Table 2.1: Partial pressure, mole fraction and maximum equivalence ratio of mixture components

Component Name	Partial pressure @ 20°C	Molar fraction	Maximum equivalence ratio (φ_{max})
Methyl acetate	170 mm Hg	0.2237	3.2
Ethyl acetate	73 mm Hg	0.0961	2.5
n-Propyl acetate	25 mm Hg	0.0329	1.06
n-Butyl acetate	1.3 kPa	0.0128	0.49
n-Amyl acetate	4 mm Hg	0.0053	0.24
Oxygen	159.2 mm Hg	0.2095	-

2.6 Experimental setup

The experimental setup of the heat flux method to be used in this project is shown in Figure (2.3).
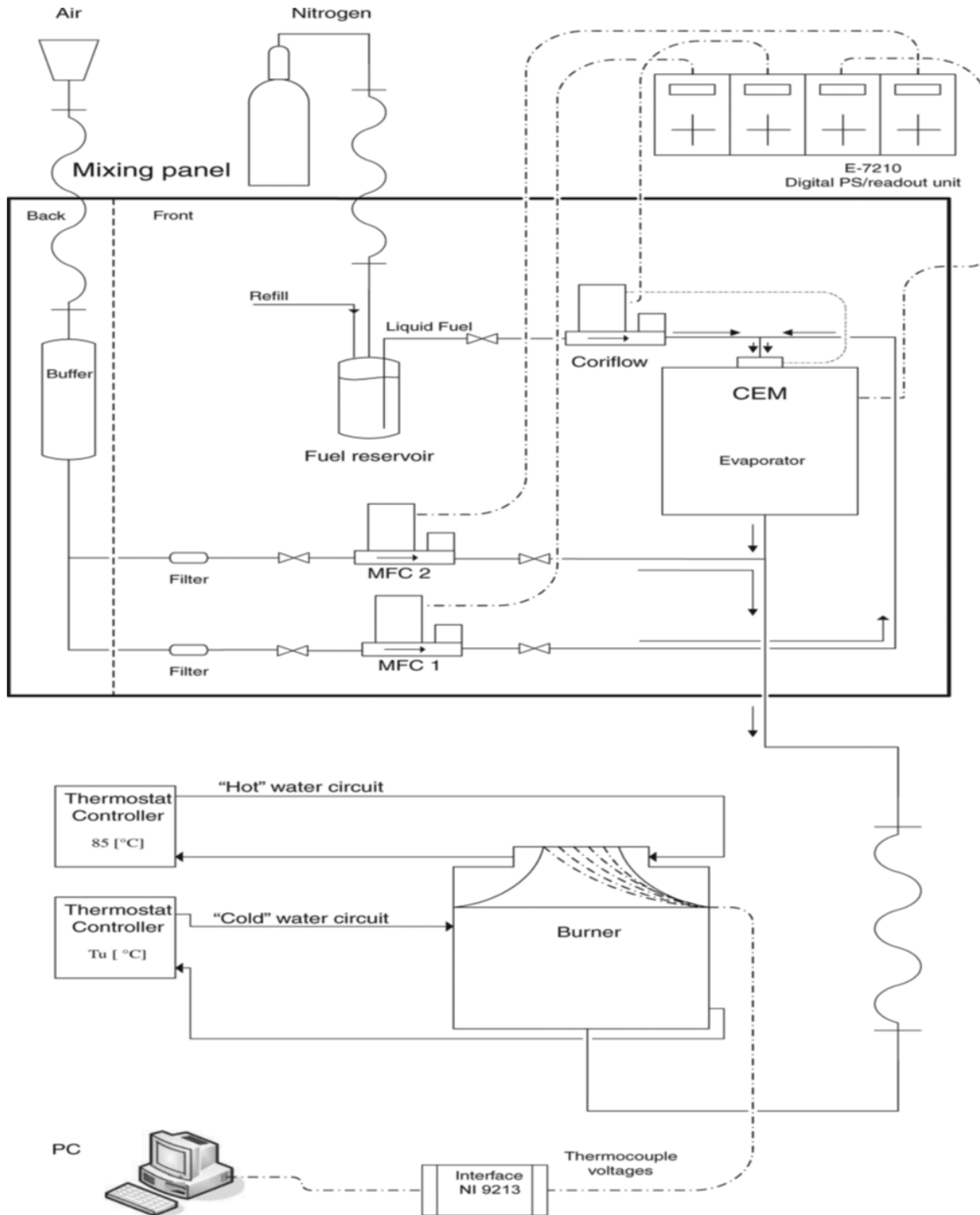

Figure 2.3: Schematic representation of the experimental heat flux method for liquid fuels from [18]

The setup consists of the following main components depicted in Figure (2.3); a short description of each part will be presented in this section, more details can be found elsewhere [14, 19].

• The burner can be considered as the main part of the heat flux setup. The burner is divided into the three essential parts: plenum chamber, burner head consists of the perforated plate which is the core of the heat flux setup and thermocouples attached to it. The perforated plate design with very small holes aims to stabilize the flame and to carry thermocouples. The thermocouple wires are carried inside small brass tubes (the same material of burner plate) with the same dimensions as burner plate hole. The perforated plate is designed in a way to force the mixture flow into the uniform flow profile after passing into the burner plate. The flame creates a pressure drop to help the mixture flow motion to become flat for high range of flow velocities. The diameter of the perforated plate holes depends on the flow velocity and therefore the range of the burning velocities can be determined. The dimensions of the perforated plate in current burner are 2 mm thickness, 0.5 mm hole diameter and 30 mm perforated plate diameter. De Goey [20] calculated numerically the range of burning velocity (10-50) cm/s for current perforated burner plate dimensions and van Maaren [13] proved that experimentally using Laser Doppler Velocity (LDV).

The principle of the heat flux method depends on the temperature difference between the burner plate and burner plenum chamber based on the heat transfer principle. To keep the temperature difference between burner head and burner chamber thermostat baths are used. The temperature of the plenum chamber is controlled by the cooling jacket at required temperature assuming that the temperature of the unburnt gas mixture equals the temperature of the burner chamber through passing it. The burner plate is kept at constant temperature (368K) using a heat jacket all the time in this work.

The last thing to be mentioned in the burner discussion is the temperature readout mechanism. The temperature distribution on the burner plate is measured by thermocouples distributed at different radial places. The thermocouples used in this setup are typed T (Copper – Constantan) wire. The diameter of the thermocouple wire is 0.1 mm chosen in this size to avoid the disturbances to the flow profile in the orifice. The physical principle of the thermocouple measurement is based on the voltage difference due to the variation of temperature between two different metals. More details about physical principles of thermocouple reading can be found in the van Lipzig thesis [15].

• The Mass Flow Controllers (MFC's) are fixed on the mixing panel and depicted in figure (2.3). The MFC is used to operate liquid/air flow in liquid heat flux installation. The liquid fuel is stored in the fuel reservoir. The fuel reservoir connects with a pressurized nitrogen line to imply a flow and to protect the fuel from moisture contamination. The nitrogen gas is used in this case because it is an inert gas. The liquid fuel flow is measured by using a mass flow meter (Cori-Flow) which connects to the Controlled Evaporator Mixer (CEM). The CEM converts the fuel to

small droplets and mixes it with a carrier gas (air in this project). It also regulates the flow depending on the feedback from Cori-Flow to obtain desired mixture composition. The mixture is heated up during flows through the high temperature spiral coil; the temperature should be sufficiently high to vaporize all liquid fuel droplets. The maximum temperature of the spiral coil is 483K. The working principle of CEM and Cori-Flow is based on the magnetic force and the Coriolis Effect respectively. More details about CEM and Cori-Flow can be found in thesis of Meuwissen [14].

The air flow is controlled by using another type of Mass Flow Controller (MFC). The working principle of this kind of MFC is based on the temperature difference of gas flows of two channels inside MFC; for more details see [21]. A buffering vessel is placed ahead of MFC's to damp pressure oscillations caused by the compressor. Also, the MFC has reduced the pressure from 3 bar to atmospheric pressure when the air passing through it. The air exiting the buffering vessel is divided into two separate channels. The first MFC provides CEM directly with required air. The second MFC connects with mixture line after the CEM output to provide air needed to obtain the gas mixture composition.

For obtaining good accuracy in laminar burning velocity, MFC's are calibrated shortly before real measurements carried out to reduce the uncertainty, more details can be found in Chapter 3, calibration process discussed in details. In this way the uncertainty will be fixed around 1% for each MFC. To keep the uncertainty in this certain point the MFC's should be used in range above 10% of their maximum flow rate.

•   The last important part in this setup discussion is readout instrument. In this work International Instrument 9213 (NI 9213) is used corroboratively by Bronkhorst High-Tech. NI9213 is used as an interface connection between user and all setup instruments depicted in Figure (2.3). All parameters related to laminar burning velocity calculations can be set manually in the Labview program to control MFC's of the required flow and to ensure correct flow calculations carried out, more details can be found in [15].

2.7 Error Sources

In this section uncertainties of laminar burning velocity are mentioned. The major sources of the experimental uncertainties in the heat flux method to determine adiabatic burning velocity can be divided into the three main error types: uncertainty of temperature profile measurement related to the irregular thermocouple placement on the burner plate, uncertainty in the liquid / air flows measurement related to the mass flow controllers and uncertainties related to the experimental procedures.

- The first type of error is created by different height of each thermocouple on the burner plate. The variation of thermocouples height creates systematic deviation of the temperature gradient of each thermocouple reading. This variation of temperature

gradient impacts estimation of parabolic coefficient (α^2) and temperature polynomial fit. Van Lipzig [15] defined the difference between thermocouple reading and temperature polynomial fit as error to fit. As sequence, standard error of parabolic coefficient (σ_{α^2}) can be determined from temperature variation of thermocouples readings to estimate α^2.

In the heat flux method the adiabatic burning velocity is determined by the interpolation from the variation between velocities around adiabatic velocity and parabolic parameter α^2 of each velocity. A linear relation between these two variables is found. From this linear relation the sensitivity of the parabolic coefficient (s) is defined as the slope of this relation:

$$s = \frac{d\alpha^2}{dS_L}\bigg|_{\alpha^2=0} \text{.. Eq. (2.12)}$$

Now to connect all this discussion with main certain point of this project (S_L), the uncertainty of the adiabatic burning velocity is defined as a combination between parabolic coefficient error (σ_{α^2}) and sensitivity (s).

$$\sigma_{SL} = \frac{\sigma_{\alpha^2}}{s} \text{.............................. Eq. (2.13)}$$

More details about this type of error can be found in references [14, 15, 16].

- The second type of error is distinguished here as uncertainty of liquid/air flows of mass flow controller. The mass flow controllers with air flows and Cori-Flow with liquid flow control the equivalence ratio and unburned mixture velocity. Therefore inaccuracies will occur from a combination of both flows. Bronkhorst High-Tech provides inaccuracies for each device will be used in this work.

Table 2.2: Uncertainties of mass flow controllers

Mass flow controller	Fluid	Uncertainty
MFC1	Air	0.8% deviation of actual setpoint, including 0.2% deviation of max. flow
MFC2	Air	0.8% deviation of actual setpoint, including 0.2% deviation of max. flow
Cori-Flow	Liquid fuel	0.2 deviation of actual setpoint

Mass flow controllers have to be calibrated shortly before starting measurements to obtain desired uncertainty estimated by manufacturer. The mass flow controllers are used in range above 10% of their maximum MFC capacity to keep the uncertainty around 1%, as recommended by Bronkhorst. By combining air flows and fuel flow, the total absolute equivalence ratio is given:

$$\Delta\varphi = \varphi\sqrt{\left(\frac{\Delta q_{MFC1+2}}{q_{MFC1+2}}\right)^2 + \left(\frac{\Delta q_{Cori-Flow}}{q_{Cori-Flow}}\right)^2} \text{.. Eq. (2.14)}$$

The uncertainty of flow influences directly the uncertainty of burning velocity calculations. Mewissen [14] determined the uncertainties of equivalence ratio and burning velocity due to mass flow controller deviation ($\pm$ 1.2%, around $\pm$ 0.42 cm/s) respectively. Similar setup will be used in this work and therefore these values can be used here also.

- Uncertainties related to experimental procedures and setup; these errors can be divided as:
    1. Fuel purity due to the solubility of nitrogen and hygroscopic nature of the liquid fuel. Meuwissen [14] carried out an experiment of burning ethanol to investigate the influence of nitrogen solubility on burning velocity and equivalence ratio, the conclusion was nitrogen solubility has no effect on burning velocity calculations. In the same thesis of Meuwissen water dissolvability calculated in ethanol during refilling liquid tank. He proved the hygroscopic nature could be considered negligible too.
    2. The influence of CEM operating temperature: this type of error investigated in details in Meuwissen [14] thesis, the experiment in this issue shows the uncertainty of adiabatic burning stays constant around $\pm 0.05\ cm/s$ if the operating temperature exceeded the fuel boiling point plus 10 ℃ and more. In the current work the CEM operating temperature is fixed at 423K.
    3. Flame structure:
    During laminar burning velocity measurements, different flame shape and structure appear depending on the equivalence ratio, unburned mixture velocity and fuel type. During measurements care has to be taken of the flame structure and shape. In this work just stable flat flames have been acceptable. Any velocity recorded not to follow these conditions is discarded, for example; unstable, cellular and not flat flame is left out of laminar burning velocity calculations. Van Lipzig [15] explained more about this topic.

Chapter 3

Calibration

3.1 Introduction

Before starting the experiment of flame burning velocity mass flow controllers are recommended to be calibrated in order to ensure maximum accuracy. In this chapter calibration of two mass flow controllers is discussed. The motivation of this calibration is elucidated. Short description of rotor meter and piston meter work is explained. After that the calibration procedure and measurements are described and errors and results are presented.

3.2 Motivation

The goal of this calibration process is to verify the mass flow rate given in the calibration certificate within the real mass flow found in a laboratory. In other words verify mass flow controller (MFC) accuracy as the relation between mass flow controllers with mixture composition, equivalence ratio and flow velocity. All of these components influence the laminar adiabatic flame velocity. As well, the second goal of MFC calibration is to find polynomial coefficients of the flow equation to set the corresponding flow with desired outflow. The calibration of each MFC is already done with air by manufacturer but this process is just to check this result. In addition, the accuracy should be good enough in the combustion process to be sure the right amount of each component is used.

3.3 Experimental Setup

3.3.1 Piston meter

Different equipments are used to calibrate the mass flow controller. Rotor meter, piston meter, compressed air and computer programs are used to operate air flow rate. Two of these equipments will be described.

Piston meter consists of a straight cylinder and piston in measuring cell. There are two junctions in this device connecting with flow fluid pipes. Inlet connects with pressure fitting while outlet connects to suction fitting pipes. The pressure will cause the piston to rise in the cylinder and give a pressure reading. The pressure reading, temperature and volume (under piston in an enclosed tube) are used to measure the volumetric flow rate by dividing the measured volume over time [22].

3.3.2 Rotor meter

The rotor meter is a mechanical device which consists of a drum, divided into four chambers. The drum is able to rotate around its axis easily and a fluid has to be approximately half filled; this fluid is called 'Packing liquid'. The packing liquid has two functions: it seals off the active measuring chamber and defines the volume of the measuring chamber by knowing the liquid level inside it. The same packing liquid which the meter is calibrated for must be filled inside it to obtain high accuracy [23].

The gas to be measured enters the drum at the inlet port, as it fills a section; it displaces the fluid allowing the drum to rotate. When the chamber is filled the inlet will be sealed by the fluid. The inlet port to the next section then opens allowing the drum to continue to rotate. As it rotates the fluid enters the first section and the trapped gas is expelled through the outlet. Based on this principle, when the drum has been calibrated after one revolution the gas volume can be known [24].

The pressure and temperature of the measured gas in this type of technology operate under ambient conditions. Under controlled conditions an uncertainty of reading as low as $\pm$ 0.2% can be achieved [24].

3.4 Method

Each MFC calibrated for one particular gas called normal gas (the gas for which the MFC is bought and calibrated with). MFC manufacturer uses air to calibrate all MFC's. In contrast, if MFC is used for another gas, it is still calibrated with air by manufacturer but corrected with conversion factors and given as a final result in calibration certificate. The error bar could be slightly different than expected due to use of different gas than normal gas, the one MFC designed for. In this project air flow is controlled using a percentage of MFC full scale to set volume flow instead of using a set of mass flow.

MFC is calibrated with rotor meter, piston meter, and high resolution camera and computer programs are used to operate air flow and set time interval between each photo and save them.

Temperature and pressure are determined during air flow measurements. Temperature is determined at different time for each flow set. The atmospheric pressure is obtained using forecast [17] internet website, where the pressure is given for each hour during the day.

3.4.1 Calibration Procedures

In this section the calibration procedures are described and a list of instructions is mentioned to follow it during the measurements.

1- Before starting taking photos and measurements
  a- Connect the certain MFC with compressed air pump passing through the drum and continue with piston meter.
  b- Make sure there are no leaks in the system and the right valves are opened.
  c- Warm up MFC at least half hour to obtain high accuracy before using it, as recommended by the MFC instruction manual [25].
  d- Check the packing liquid level inside the drum; it should be approximately half filled. Also, the packing liquid should be the same as the meter is calibrated with to obtain high accuracy.
  e- Apply compressed air or any pressure to the rotor packing liquid inside the drum.
  f- Choose arbitrary different flows to be set in the flow view program.
  g- Set the percentage needed or volumetric flow and wait 1-2 minutes before taking any photo.
  h- Calculate time interval for each set flow to be set in Timershot program.
2- Taking photos
  a- Check the pressure using forecast website [17] each hour. It is recommended to check the pressure meter in another lab to see the pressure variation during the day. In this calibration process pressure obtained from internet is reliable.
  b- Register the temperature using thermocouple fixed in the outlet of the rotor meter. Recommended to take an average of temperature between starting and ending point.
  c- Set the time interval required for each set flow.
  d- Take seven different photos, with six different measured flows.
  e- During each photo, make sure the rotor meter uses 20 litre of packing liquid within two cycles.
  f- Before changing percentage of MFC flow to set a new set point, register average of piston meter reading.
3- New set flow
  a- If new flow is set, make sure the MFC and rotor meter get enough time to stabilize with this new speed or certain flow.
  b- Press on the reset button on piston meter board to repair it for new set flow.
  c- Repeat the same procedure in step two with this new set flow.
4- When completed all set flow points
  a- Set MFC flow back to zero.
  b- Close green valve and remove pressure from the system by turning off compressed air tap.
  c- Return web camera and piston meter in the right places and rotor meter in safe place.

d- Take the difference between each two photos to get all volumetric flow rates.
e- Fill the data in excel file in such a way that matlab can be used (csv-file) to process the data.

3.5 Calculations, Results and Errors

In the following calculations, MFC's set points are given in normal conditions (temperature of zero °C and standard atmospheric pressure). In general, any set flow will be the flow under normal conditions. In contrast, rotor meter measurements are taken under room temperature and ambient pressure. However, to circumvent this problem the following calculations will be carried out for normalizing the data and make it possible to work with volume flows. The ideal gas equation is used to convert the calculated flow rate from room conditions to the normal conditions as shown in equation (4.1) :

$$\Phi_v^{actual,0°C} = \frac{P_R * T_{0°C}}{P^{1atm} * T_R} \Phi_{v,i}^{rotor} \quad \text{.........................….… Eq. (3.1)}$$

$$\text{where } \Phi_{v,i}^{rotor} = \frac{\Delta V_i}{\nabla t_i} \quad \text{…........................…... Eq. (3.2)}$$

Φ_v^{actual} is the actual volume flow calculated in normal conditions, P^{1atm} is the standard atmospheric pressure (at 1atm). Room pressure and temperature are signed by subscript R (room), T is the temperature and the subscript 0 represents normal condition at zero °C. Also, $\Phi_{v,i}^{rotor}$ is the volume flow measured with the rotor meter, ΔV is the difference in volume and Δt is the difference in time corresponding to the volume difference. The index i stands for the different measurements.

Actual volume flow calculated in equation (3.1) is compared with the corresponding set flow; these flows should be identical with each other in ideal cases. Error flow is defined as the difference between actual flow and corresponding set flow. An error is calculated by using equation (3.3):

$$Error_i = \frac{\Phi_v^{actual,0°C} - \Phi_v^{set,0°C}}{\Phi_v^{set,0°C}} \quad \text{…....................….... Eq.(3.3)}$$

where $\Phi_v^{set,0°C}$ is the arbitrary set flow representing the volumetric flow rate in normal conditions.

The error bars are obtained by taking the mean and standard deviation of errors for different measurements of each set flow, using the following equations.

$$\bar{x} = \frac{1}{n} \sum_{i=1}^{n} x_i \quad \text{…........................….... Eq.(3.4)}$$

$$s = \left(\frac{1}{n-1}\sum_{i=1}^{n}(x_i - \overline{x})^2\right)^{\frac{1}{2}} \quad \ldots\ldots\ldots\ldots\ldots \text{Eq.(3.5)}$$

where n is the number of measurement points and index i stand for different measured points. In the following, figures with error bars are shown and discussed for each MFC with drum and piston data. Also, a polyfit function and Figures are presented; as well, numerical values of polynomial coefficients are given in a Table 3.1.

Figure 4.1 below represents the error bars of the data obtained using a rotor meter (blue and light blue lines) and piston meter (green, red and purple lines). The Figure shows MFC flow curves at each set point used in piston meter and rotor meter, in this calibration also error bars attached with it. Each flow curve in this figure approximately has its own behaviour without general common trend. The calibrations were repeated many times to obtain accurate results. The reason for the different curvatures is unknown but could be related to turbulence of the rotor flow rate during the measurement procedure. MFC calibration is considered not to be accurate enough because of no common behaviour between these curves and also the big error bars; for example, at the light blue line in the third error bar exceeds 1%.
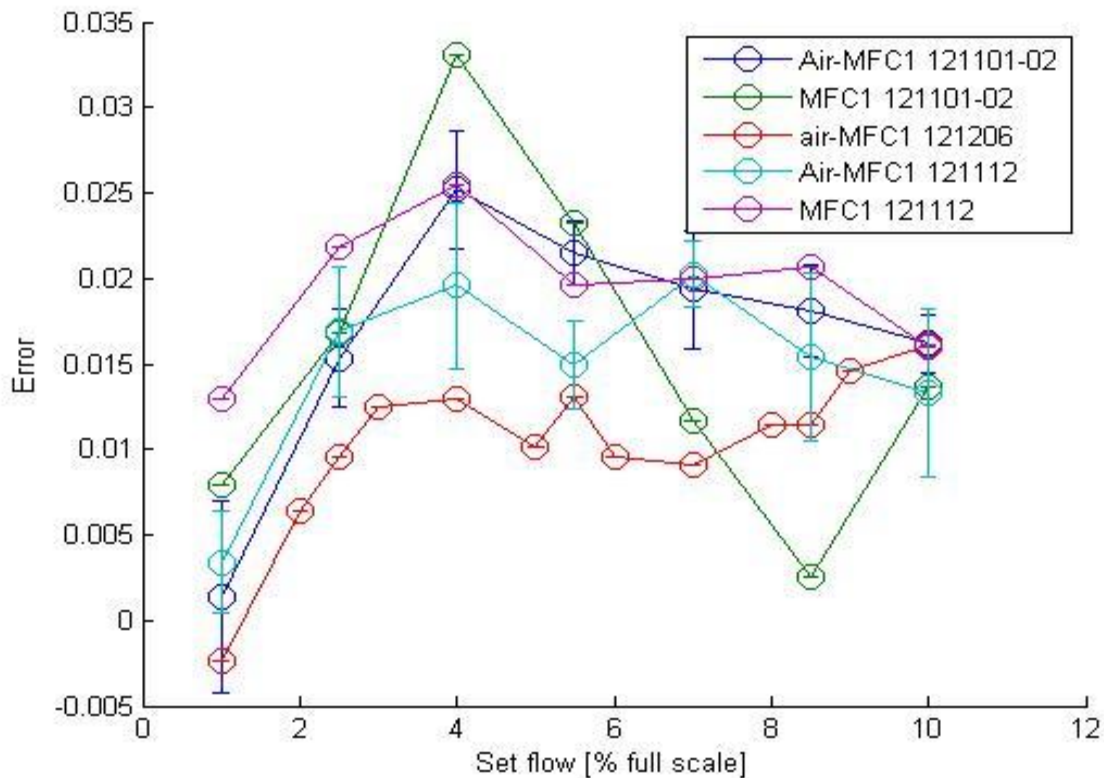

Figure 4.1: Air MFC error bars for different flows measured with rotor (blue line) and piston (green line)

Error in the second N2 MFC is shown in Figure (2) below. The behaviour in this MFC is considered to be accurate enough because the new results have the same curvature as compared to old results; also, the drum error bars are less than 1%.
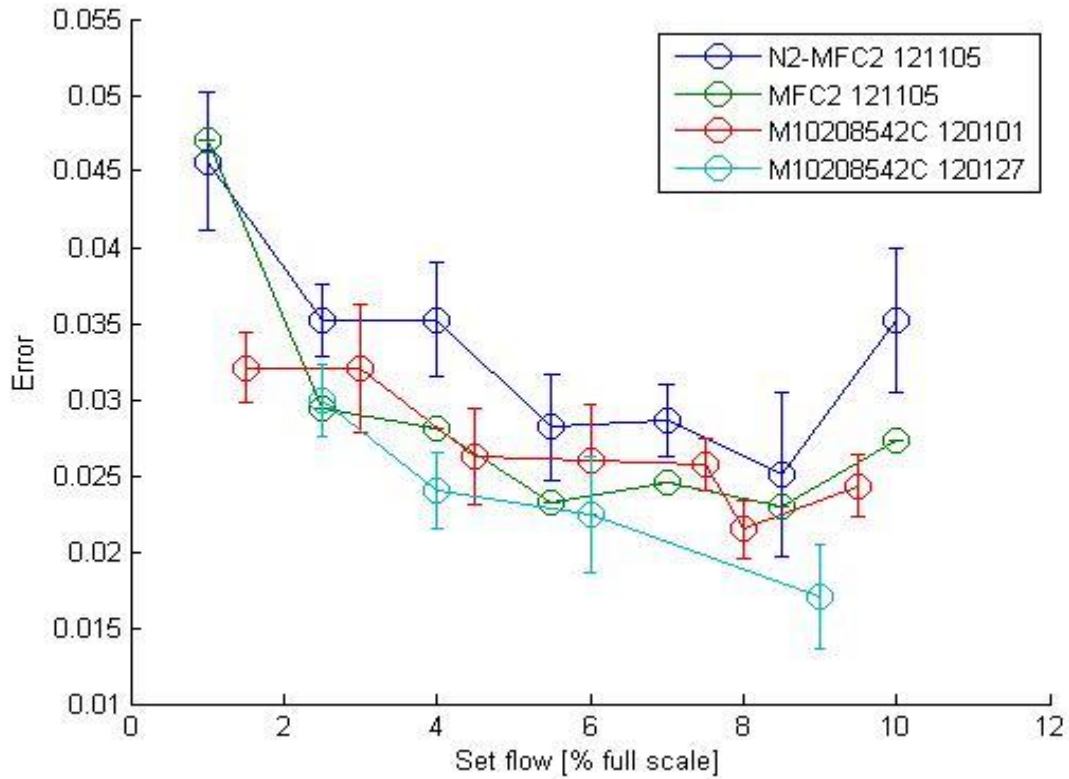

Figure 4.2: N2 MFC error bars for different flows measured with rotor (blue line) and piston (green line)

Figures number 3 and 4 below show the experimental points and fit line of these points. Fit line means that there is minimum uncertainty and set flow corresponding to the measured flow as used as possible. These two fit lines are taken from rotor meter data because the measured flow with this instrument is considered more accurate than piston meter.
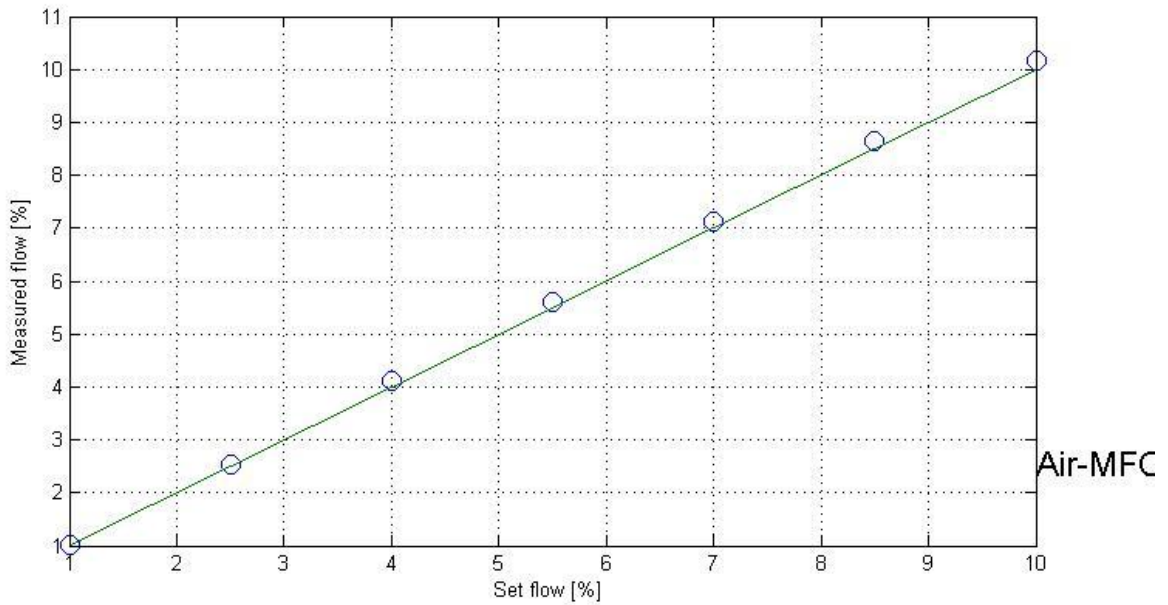
Figure 3: Air MFC polyfit between the actual flow (*y*-axis) and set flow (*x*-axis)
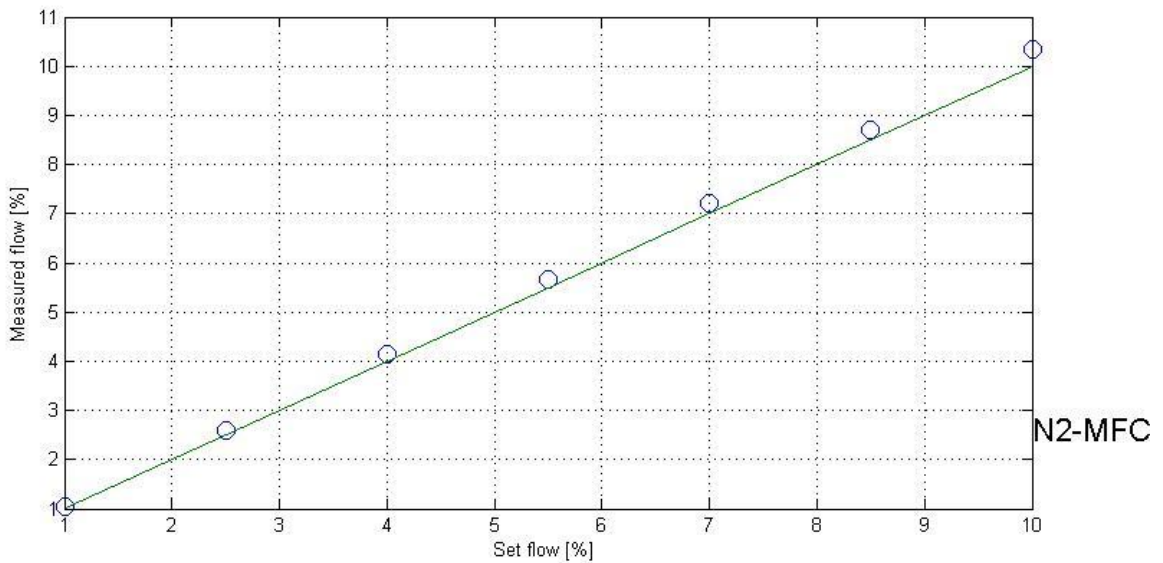

Figure 4: N2 MFC polyfit between the actual flow (*y*-axis) and set flow (*x*-axis)

 The list of polynomial coefficients is tabulated below, including for each MFC four rows of coefficients. Two of them are represented the direct and inverted coefficients of rotor meter and the other two for piston meter. The fourth degree polynomial is suitable to fit these experimental data. The coefficients are used in the equation (4.6) to fit the measured flow corresponding to set flow.

$$\Phi_{set} = a_1 \Phi_{measured}^4 + a_2 \Phi_{measured}^3 + a_3 \Phi_{measured}^2 + a_4 \Phi_{measured} + a_5 \ \text{........} \ \text{Eq.(4.6)}$$

where Φ_{set} is the set flow, $\Phi_{measured}$ is the measured flow and the coefficients from a_1 to a_5 are the calibration coefficients to be used and filled in the specialized program to obtain certain flow.

Table (3.1): list of direct and conversion polynomial coefficients for fourth polynomial fit

Air-MFC1 (121101-02)_dir(Rotor)	0.0001	-0.0014	0.0074	1.0167	-0.0231
Air-MFC1 (121101-02)_inv(Rotor)	-0.0001	0.0013	-0.0074	0.9847	0.217
Air-MFC1 (121101-02)_dir(Piston)	0.0007	-0.0143	0.0862	0.8454	0.0888
Air-MFC1 (121101-02)_inv(Piston)	-0.0007	0.0139	-0.0857	1.158	-0.0928
N2-MFC2 121105_dir(Rotor)	0.0003	-0.0049	0.0281	0.9698	0.0530
N2-MFC2 121105_inv(Rotor)	0.000268	-0.00489	0.028093	0.969765	0.052987
N2-MFC2 121105_dir(Piston)	0.0001	-0.0017	0.0105	0.9961	0.0421
N2-MFC2 121105_inv(Piston)	-0.0001	0.0015	-0.0096	1.0029	-0.0412

Lastly, these polynomial coefficients, atmospheric pressure and temperature of unburned gas mixture will be applied in the Labview program mentioned in Chapter 2 section 2.4 to verify the desired flows by mass flow controllers before start of taking measurements in the laboratory.

Chapter 4

Results and Discussion

4.1 Introduction

Laminar burning velocities of esters/air flames are measured using the heat flux method described in Chapter 2 at atmospheric pressure, variable unburnt gas mixture temperature from 298 K to 348 K for several equivalence ratios from 0.7 to 1.5. The maximum limit of equivalence ratio depends on the experimental conditions to get stable flat flame.

The first plan in this study mentioned in Chapter 1 is to provide experimental results of five esters fuel selected with straight carbon chain length C3-C7. In this study, the last two fuels (n-butyl acetate and n-amyl acetate) were not possible to combust in the current experimental setup due to partial pressure limitations described in section 2.5. Therefore, new ester fuels with a lower molecular mass are selected to complete this experiment instead of burning unsuccessful fuels. However, some results obtained during burning methyl formate are not acceptable. This is because the required fuel mass flow to attain the laminar burning velocity exceeded the upper limit of the fuel mass flow controller. Also, the control evaporator mixer suffered from contamination with this aggressive fuel. As a result, for these reasons the current project sufficed for determining burning velocities of methyl acetate, ethyl acetate and n-propyl acetate. The numerical values of all experimental laminar burning velocities determined in the present study are tabulated in Appendix A.

4.2 Laminar flame speed of esters at different temperatures from 298 K to 348 K

Laminar flame speed of methyl acetate, ethyl acetate and n-propyl acetate have been determined using the heat flux method at different temperatures as a function of equivalence ratio. In this section all results are presented in Figures 4.1-4.3 and compared to each other. There are limited literature available for these fuels to compare with it (Figure 4.2); on the other hand, a related ester study presented in Table 1.2 operated at different combustion conditions or different chemical structure combined with existing relevant results in Figures 4.4 and 4.7 is used as a guide for validity and reliability of current results. Also, the fuels with the same carbon number (methyl butanoate) and the same alkyl group (methyl formate) taken from the literature Table 1.2 are used to discuss the carbon chain length effect on laminar flame speed.
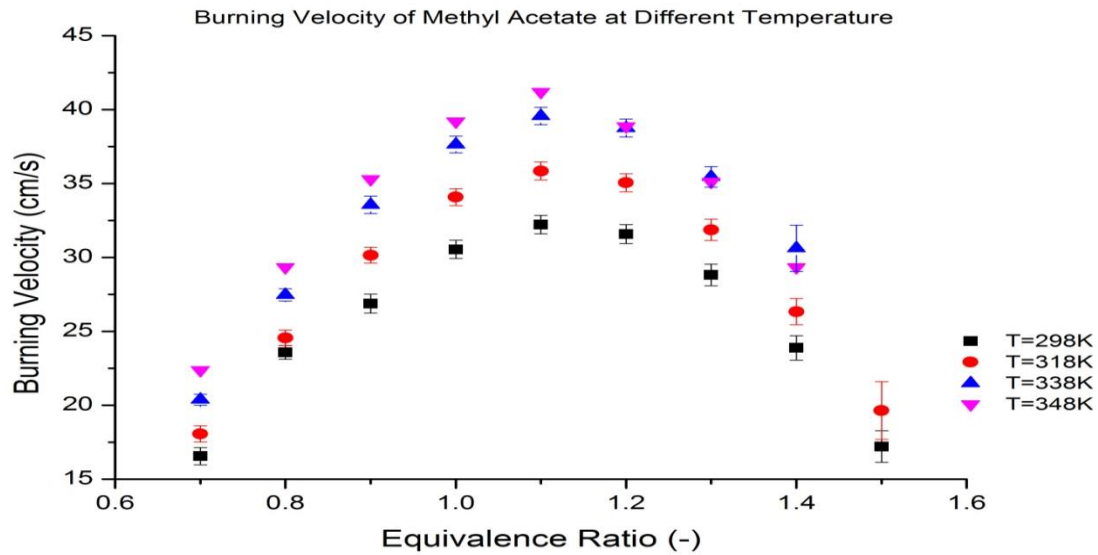
Figure 4.1: Adiabatic burning velocity of methyl acetate at $298\,K - 348\,K$

Figure 4.1 shows the burning velocity of methyl acetate at different initial temperatures. The flame speeds increase with inlet pre-mixture temperature as expected. Most measurements had been repeated separately, the differences were measured within experimental uncertainty range. In all experiments the curvatures at all temperatures are similar to each other, also the maximum burning velocity is reached at equivalence ratio $\varphi = 1.1$. Overlapping the results at $(T = 348\,K)$ with lower temperature results $(T = 338\,K)$ is observed at a higher equivalence ratio $(1.3 - 1.4)$. The results at $348\,K$ were measured in a different thermocouple connection; had large uncertainty ranges. It was found that the thermocouple connection used for $298 - 338\,K$ results gave smaller uncertainty and was therefore used. The error analysis method discussed in Chapter 2 is used to estimate error bars instead of Meuwissen [14] procedure. The redetermined burning velocities at different temperature prove good resemblance with old results. Due to use of all the fuel before remeasuring the flame speed at all temperatures, the results at $T = 348\,K$ of methyl acetate and also for n-propyl acetate are still acceptable results. The intersection between these two results mentioned above ($338\,K$ and $348\,K$) could be related to thermocouple connections used during recording these measurements at temperature $(T = 348\,K)$; however it is still within uncertainty range. The results presented in Figures $(4.1 - 4.3)$ can be assumed with a higher level of accuracy, less than $\pm 1\,cm/s$, except for some earlier results at conditions mentioned above.
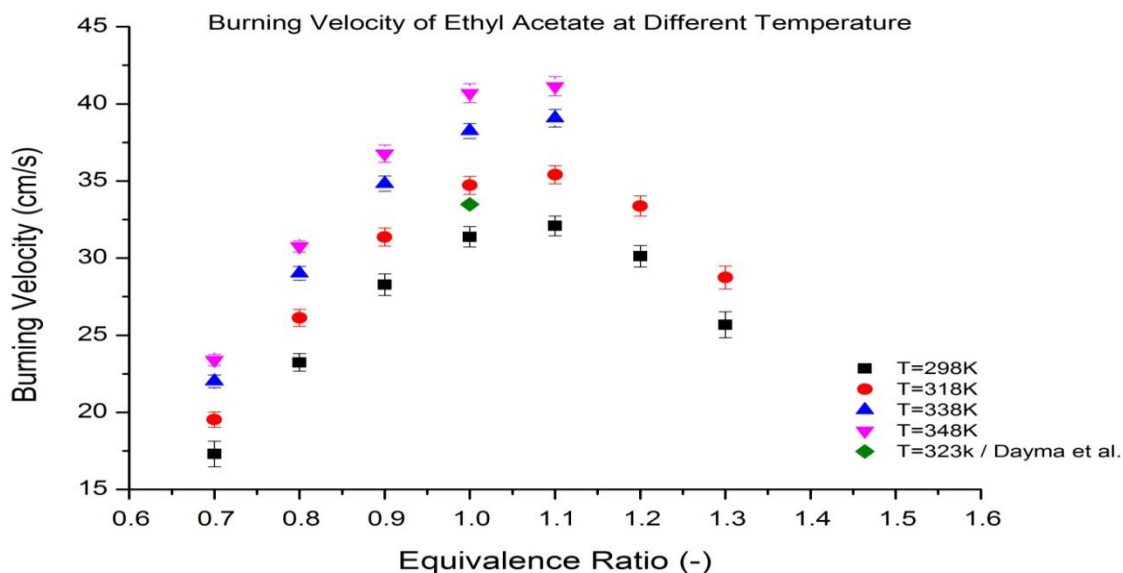
Figure 4.2: Adiabatic burning velocity of methyl acetate at $298\ K - 348\ K$
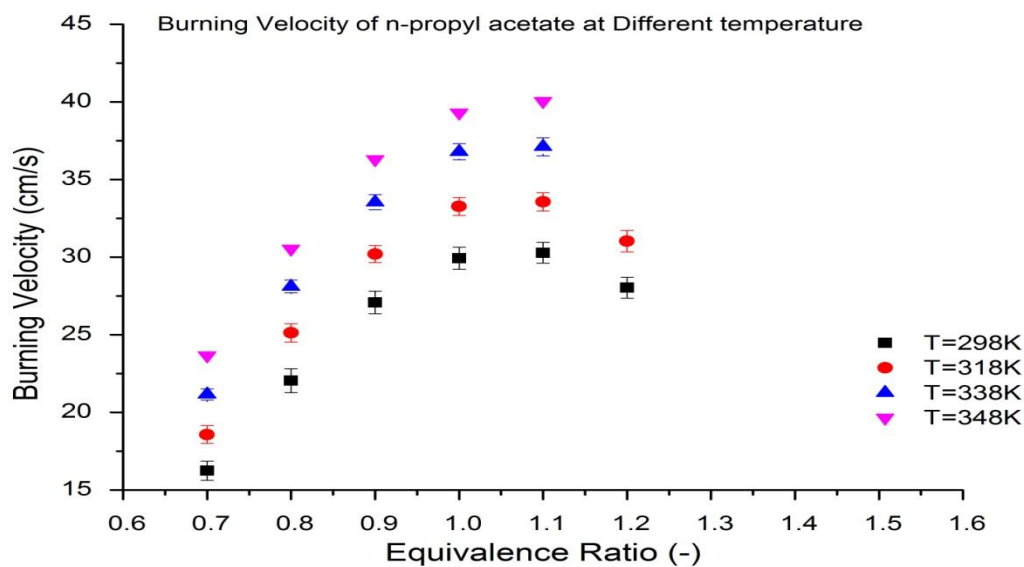

Figure 4.3: Adiabatic burning velocity of methyl acetate at $298\ K - 348\ K$

Figures 4.2 and 4.3 show the laminar burning velocity of ethyl acetate and n-propyl acetate respectively. The result of both fuels is similar and no unexpected behaviours have occurred. It is worth to mention that the maximum value of equivalence ratio is reached at lower temperature and carbon chain length. In general, there is an inverse relation between the highest equivalence

ratio at stable flat flame with carbon chain length as well as fuel molecular mass. Figure 4.2 shows Dayma et al. [9] result of ethyl acetate at experimental conditions ($\varphi = 1$ and $T = 323\,K$). This result able to compare with the current result of ethyl acetate at $T = 318\,K$. A good agreement can be found between these results with a slight increment in recent result. However, the heat flux method used in this project is assumed more accurate than spherical bomb method used in the Dayma study. The results in Table 4.1 are obtained by linear extrapolation to $\alpha^2 = 0$ instead of interpolation as described in Chapter 2 section 2.2. Extrapolation method is used in these cases because it was impossible to find stable flat flame above adiabatic conditions. The linear extrapolation is expected to yield reasonable results because these flow velocities were taken very close to the laminar burning velocity at adiabatic condition.

Table 4.1: Esters results obtained by the linear extrapolation method

Ester name	Temperature	Equivalence ratio
Methyl Acetate	338K	1.4
Ethyl Acetate	348K	1.1
n-Propyl Acetate	318K	1.2
n-Propyl Acetate	338K	1.1

4.3 Laminar flame speeds propagation with increment carbon chain at variable temperatures

The experimental results of laminar burning velocities of methyl acetate ($C_3H_6O_2$), ethyl acetate ($C_4H_8O_2$) and n-propyl acetate ($C_5H_{10}O_2$) are shown in Figures (4.4-4.7) at different temperatures. Each Figure shows the flame speed propagation for different esters at a specific temperature. Figure 4.4 combined with the burning velocity of methyl formate ($C_2H_4O_2$) of the Dooley et al. [7] study. Also, Figure 4.7 gather with Liu et al. [6] results of methyl butanoate ($C_5H_{10}O_2$) at $T = 353$ K to compare with current results. First the results will be shown and afterwards some comments and discussion follow.

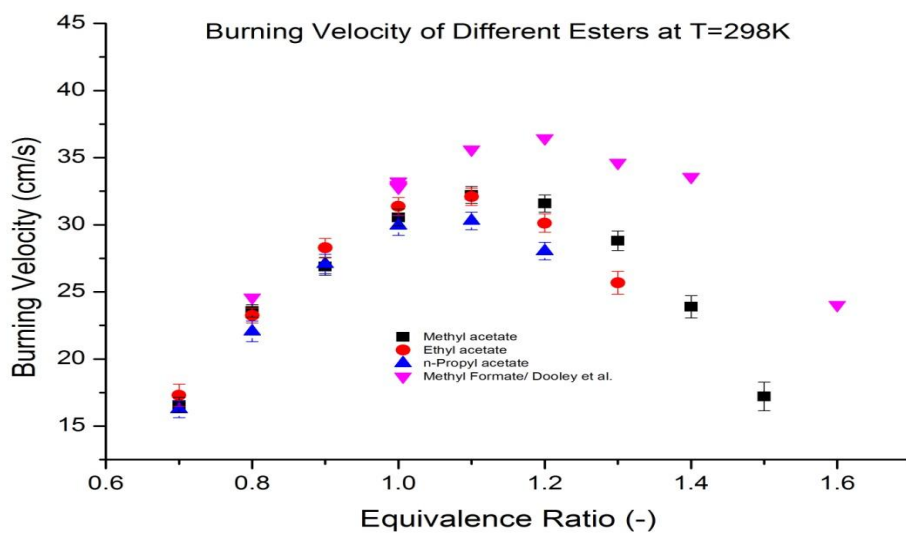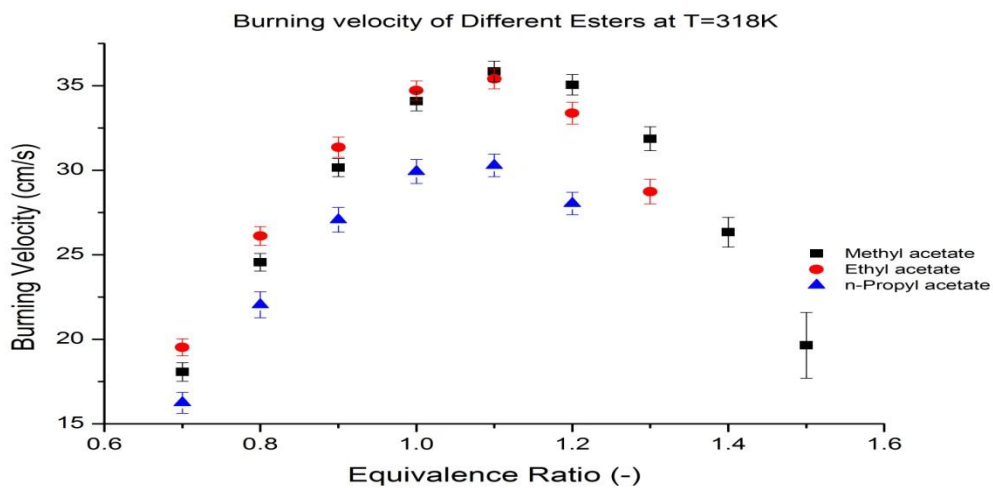**Figure 4.4:** Burning velocity propagation with increment carbon chain C2-C5 at $T = 298\,K$

Figure 4.5: Burning velocity propagation with increment carbon chain C3-C5 at $T = 318\,K$

35
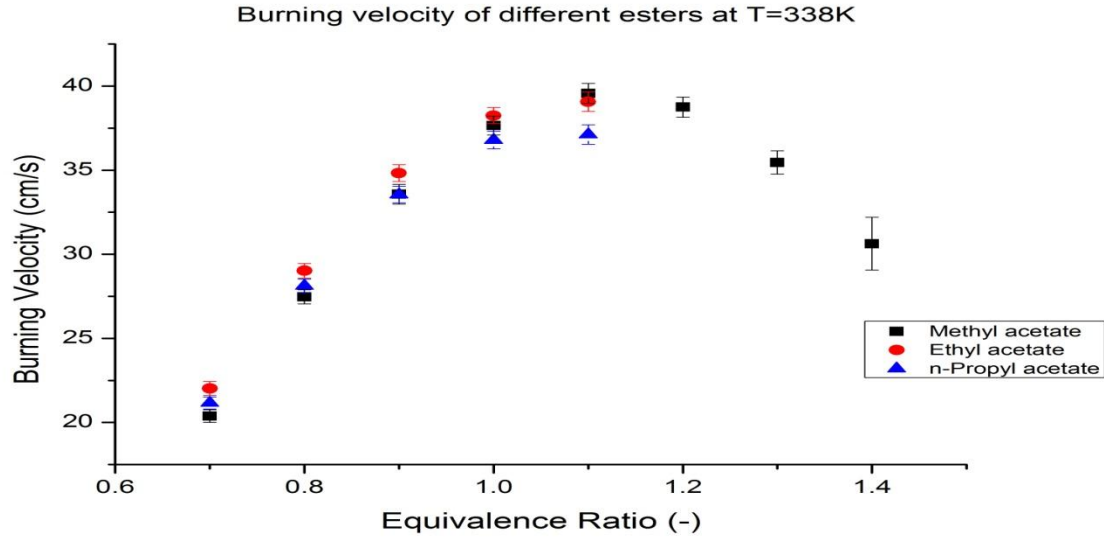
Figure 4.6: Burning velocity propagation with increment carbon chain C3-C5 at $T = 338\ K$
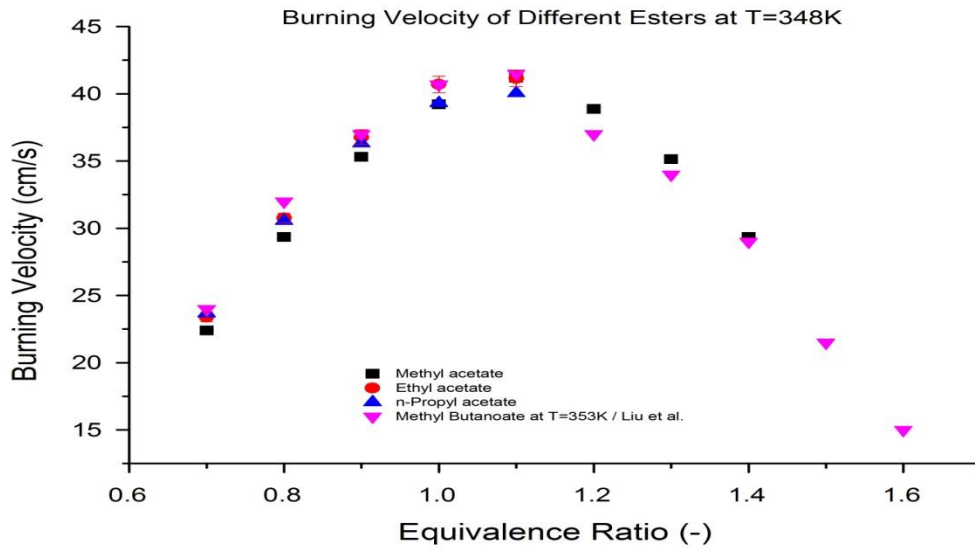
Figure 4.7: Burning velocity propagation with increment carbon chain C3-C5 at T=348K

The results show the laminar burning velocity of n-propyl acetate, ethyl acetate (EA) and methyl acetate (MA). In Figures $4.4 - 4.7$ at four different temperatures from $298\ K$ to $348\ K$. The figures show that n-propyl acetate has the lowest flame speed at all temperatures. Figure 4.5 shows that the burning velocities at temperature 318 K have maximum difference between burning velocities of n-propyl acetate compared to the others two fuels around 5 cm/s at $\varphi = 1.1$. In Figure 4.4 to Figure 4.6 the results of adiabatic flame speeds are compared with each others.

It is obvious that the laminar flame speeds follow this order n-propyl acetate $<$ ethyl acetate $<$ methyl acetate in general for all equivalence ratios but it is very clear at rich mixture. This result agrees with Wang et al. [8] result the effect of the ester group on the overall reactivity diminishes as the carbon chain increase. The overlapping results between the burning velocity of ethyl acetate and methyl acetate at $\varphi \leq 1$ can be seen in all Figures. Generally at lean mixture the laminar flame speeds of ethyl acetate is faster than the flame speed of methyl acetate. The overlapping between these fuels could be due to the similarity in the chemical structure of the small ester group or because intersection occurs within an uncertainty region or maybe due to low fuel concentration (at $\varphi \leq 1$). Figure 4.7 higher burning velocities are obtained for n-propyl acetate at $T = 348\ K$ compared to the burning velocities of lower temperature with other fuels. On the other hand, the differences of burning velocity compared to MA and EA could be assumed negligible. Approximately all the fuels at high temperature have the same speed independent of carbon chain length. In general, for each ester the maximum limit of equivalence ratio can be reached at low temperature and short carbon chain length.

No literature data exist regarding the laminar burning velocity of the same esters under study; due to that general discussion carried out with regard to similar esters with the same carbon number or with the same alkyl group to compare it with this work.

At the beginning, Figure (4.4) shows the laminar flame speed of methyl formate (MF) from Dooley at el. [7] study added to the current ester results at temperature 298 K. The Figure shows a significant difference in burning velocity between MF and the other three esters. This result reveals an inverse relation between burning velocity and carbon chain length; regarding MF it has a shorter carbon chain and faster burning velocity. The maximum difference between MF and methyl acetate is 6 cm/s. However, the difference in burning velocities for other esters are around 2 cm/s with an increment of carbon chain length (C1). The high difference of burning velocity between these fuels could be related to experimental method used in Dooley work. In the MF experiment a dual-chamber cylindrical bomb used to determine laminar burning velocity. This method depends on an extrapolation technique to estimate burning velocity. Besides this method contains experimental difficulties at rich mixture (high equivalence ratios) affecting the burning velocity estimation. Another possibility could be related to the chemical structure of MF. The chemical structure of MF very simple compares to other esters in this study. The ester group in MF connects with one hydrogen atom whereas the remaining esters connect with a methyl (CH_3) branch. The chemical combustion reaction could be using internal burning energy to break the carbon bond in the (CH_3) branch and therefore lower burning velocity can be obtained for all other esters except MF.

Dayma et al. [9] studied the laminar flame speed of ethyl esters at different experimental conditions. The strong agreement can be found between this study and the current result for ethyl acetate at temperature close to $T = 318K$. The laminar burning velocity of ethyl acetate at

($\varphi = 1$) in the present study is ($S_L = 34.72\ cm/s$ at $T = 318\ K$) whereas the Dayma study gives ($S_L = 33.48\ cm/s$ at $T = 323\ K$) as shown in Figure 4.2.

Figure (4.7) shows the burning velocity of methyl butanoate according to the Liu et al. [6] study at experimental conditions ($T = 353\ K$ and $P = 1\ atm$) combined with other ester results to compare it with n-propyl acetate at $T = 348\ K$ because they have the same carbon numbers and approximately the same temperature. The results of n-propyl acetate agree with methyl butanoate, the last one slightly higher. Both of these fuels have the same carbon number (C5). This result shows that the chemical structure has no effect on the laminar burning velocity for n-propyl acetate and methyl butanoate at long carbon chain.

4.4 Laminar flame speed of Esters compared to Alkane

Figure 4.8 shows the laminar flame speed of ester, results collected from current investigation and relevant studies mentioned before to be compared with the alkane group Ranzi et al. [26] study (C_2H_6, C_3H_8 and nC_4H_{10}) at the same carbon length (carbon numbers).
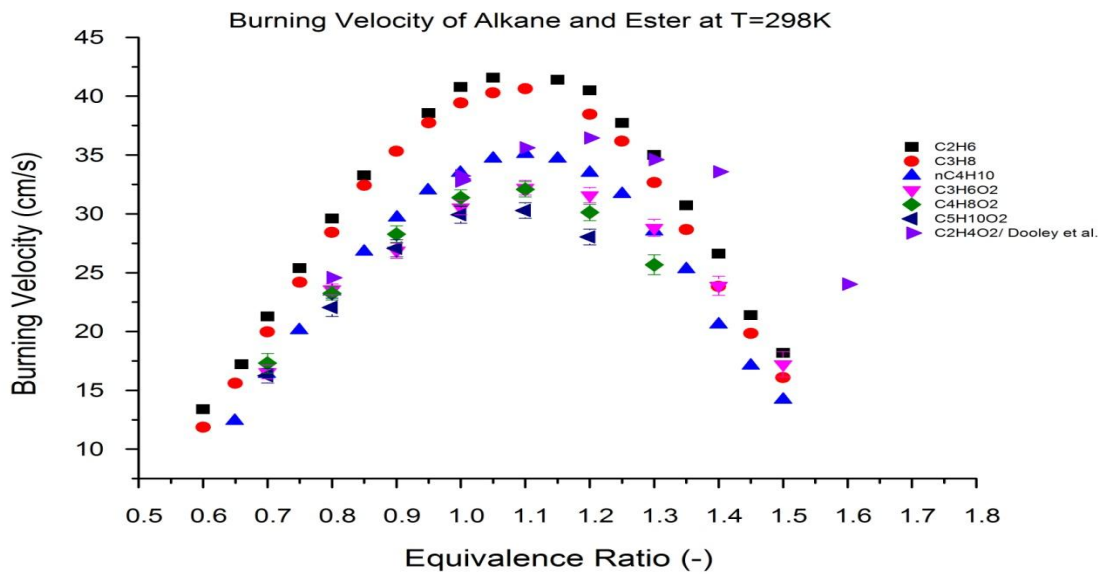

Figure 4.8: Comparison between ester group and Alkane group from Ranzi et al. [26]

The heat flux method used in the current work to determine the burning velocity of esters, and the same technique was used in alkane. The laminar flame speed of the alkane group decreases with increasing carbon chain length. The same behaviour follows in the ester group as shown in Figure 4.8. The burning velocity of the ester group behaves the same way as the alkane group as a function of carbon chain. As a result, the propagation of laminar flame speed inversely increases with carbon chain length for esters and also for alkanes. Lower burning velocities can be observed significantly in the ester group compared with the corresponding alkane group at the same carbon numbers. The maximum burning velocity of all fuels in both groups has the same

position at an equivalence ratio ($\varphi = 1.1$). In the alkane group the laminar flame speed can be measured at the rich mixture regardless of carbon chain length whereas the maximum limit of equivalence ratio in the ester group depends on that. The explanation for this could be that alkane group is found in the gas phase but the ester fuels are in liquid phase. Due to that the ester group at a higher equivalence ratio and long carbon chain suffers from condensation and this is not the case for alkane group.

4.5 Temperature correlations with laminar burning velocity

The measured laminar flame speeds of esters/air flames at atmospheric pressure and different inlet temperatures from 298 K up to 348 K for several equivalence ratios are shown in the following figures using log-log scale (4.9, 4.11 and 4.13). Experimental power exponent coefficients are determined as a function with equivalence ratio and followed after each figure. The power exponent coefficient α_T is determined by finding the slope of the temperature dependence lines with the flame speed at each equivalence ratio. The error bars of the current values are derived by averaging the error of the individual flame speed measurements at different temperatures. The uncertainty of the power exponent is very high due to the narrow temperature range; in order to increase the accuracy of α_T coefficients, the temperature range have to be extended. Figures (4.10, 4.12 and 4.14) show a power exponent as a function of various equivalence ratios for each ester used in this study.
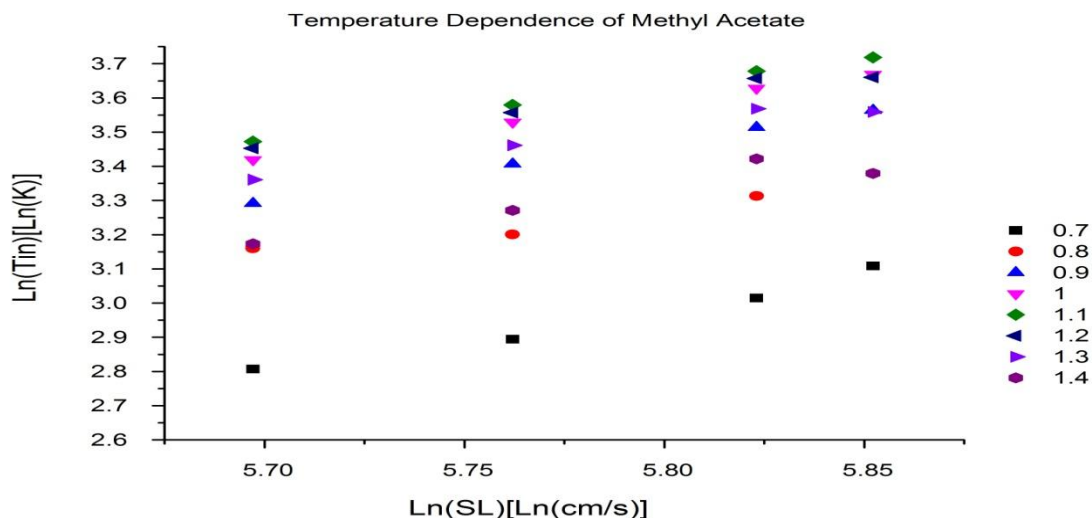

Figure 4.9: Temperature dependence of methyl acetate/air flame speed in the temperature range 298-348K

Figure 4.10: Power exponent versus equivalence ratio for methyl acetate flames

Figure 4.9 shows the temperature dependence of methyl acetate burning velocities in the temperature range $298 - 348$ K. Figure 4.10 shows the power exponent coefficient determination with various equivalence ratios. According to the experimental result the coefficient α_T shows a non-linear behaviour. A minimum coefficient value is observed at an equivalence ratio equal 0.8. Power exponent coefficients follow unexpected curvature in Figure 4.10 compared to other fuels found in literature [14, 18] which could be due to an experimental error at equivalence ratio 0.8.

Figure 4.11: Temperature dependence of ethyl acetate/air flame speed in the temperature range 298-348K
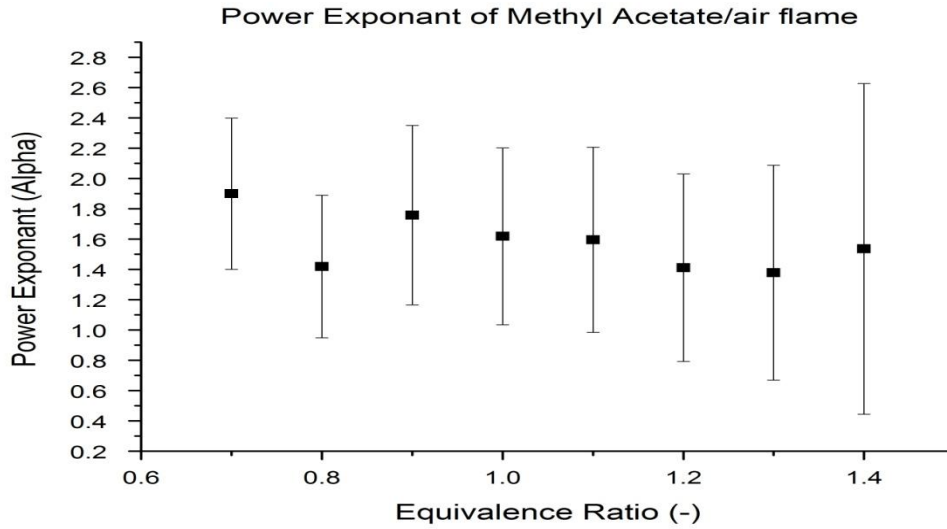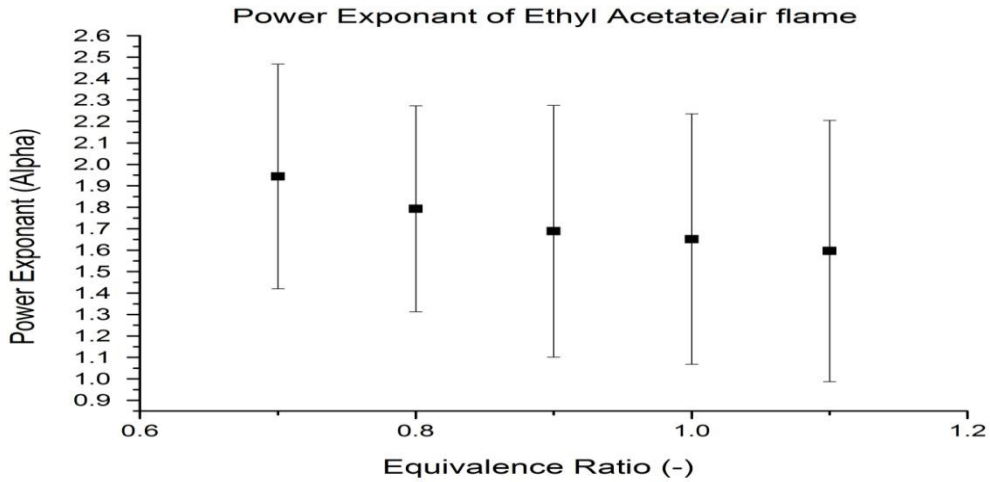
Figure 4.12: Power exponent versus equivalence ratio for ethyl acetate flames

Figure 4.11 shows the temperature dependence of ethyl acetate burning velocities in the temperature range 298-348K. Figure 4.12 shows the power exponent coefficient determination with variable equivalence ratios. According to the experimental result the coefficient α_T shows approximately a linear decrease behaviour.
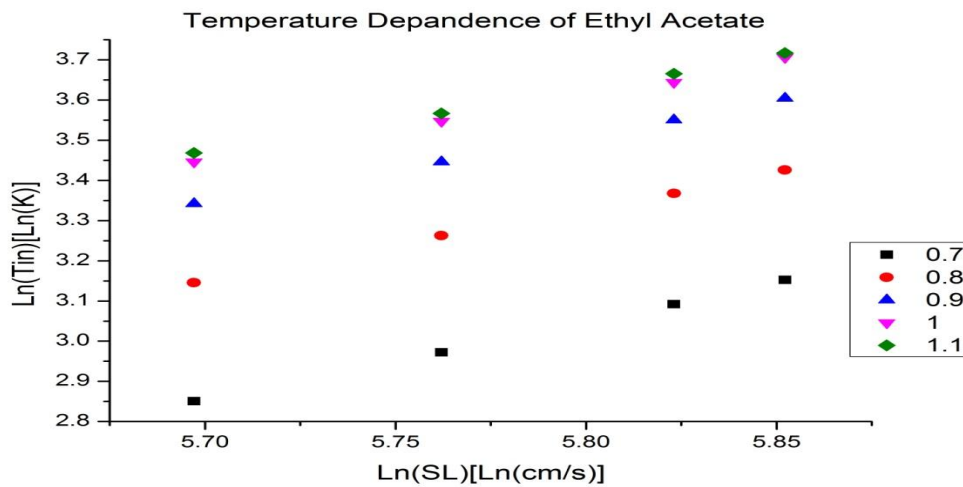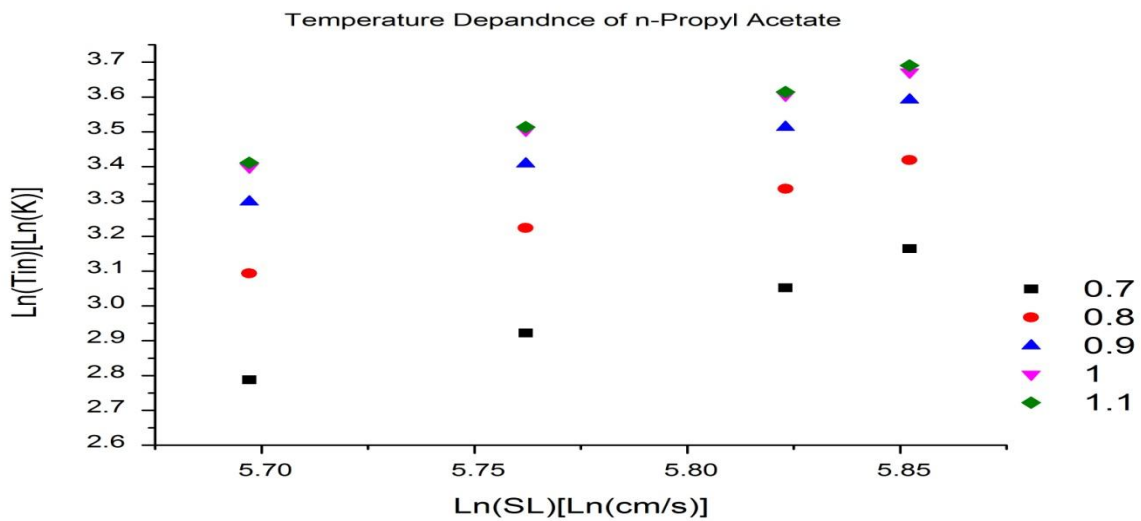

Figure 4.13: Temperature dependence of n-propyl acetate/air flame speed in the temperature range 298-348K
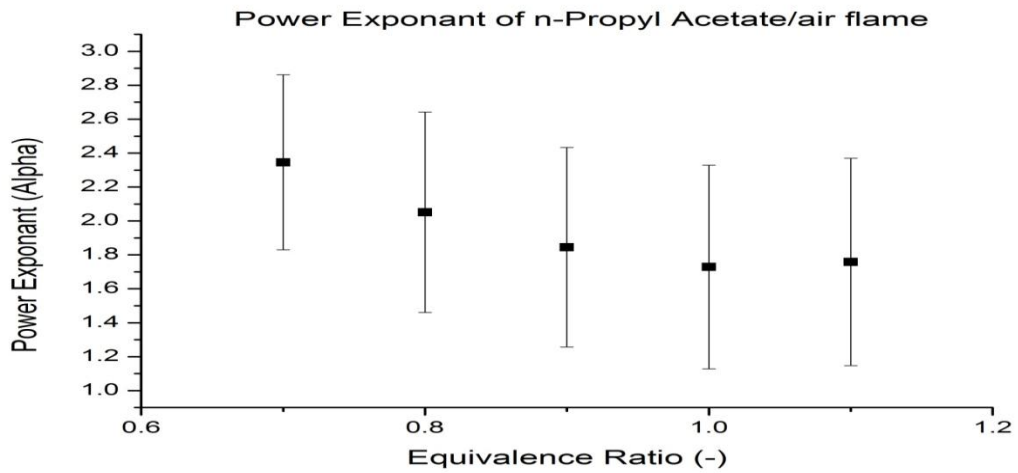
Figure 4.14: Power exponent versus equivalence ratio for n-propyl acetate flames

Figure 4.12 shows the temperature dependence of n-propyl acetate burning velocities in the temperature range 298-348K. Figure 4.13 shows the power exponent coefficient determination with variable equivalence ratio. According to the experimental result the coefficient α_T shows a non-linear behaviour (parabolic curve). A minimum coefficient value is observed at an equivalence ratio equal 1.

Chapter 5

Conclusions and Recommendations

The heat flux method is a very efficient technique to determine the adiabatic burning velocity of liquid fuel. The primary goal of this project is to provide new and accurate measurements of the laminar burning velocity of three bio-fuel (ester group). The second goal was to investigate the laminar flame speed propagation with carbon chain length from C3 to C7.

First of all and before starting experiments, two mass flow controllers were calibrated to obtain a high level of accuracy and use calibration polynomial coefficients to correct flow equation. The error in the mass flow controller is larger than what was expected by 1% and does not give the same curvature for all the different measurements. The nitrogen mass flow controller gave a reasonable systematic error of less than 1% and the curvature trend was similar to the old calibration.

Laminar burning velocities of methyl, ethyl and n-propyl acetate have been determined. The experiments are operated in a temperature range $(298K - 348\ K)$ of unburned fuel/air mixture. An attempted range of equivalence ratio was from 0.7 to 1.5; however, depending on experimental conditions some rich mixtures were not accessible for measurements. The highest possible burning velocity was obtained at an equivalence ratio of 1.1 for all temperatures and esters under study. The overall accuracy of the burning velocities was estimated to be around $\pm 1\ cm/s$. The temperature dependence of the unburned mixture on laminar burning velocity is studied and the power exponent for several equivalence ratios is determined and presented for each ester.

The burning velocities of esters/air flames were compared with respect to each other because there are no literature data available to compare with. A comparison was done for flame speeds of each ester at different temperature and the flame speeds for all esters at a specific temperature. The result obtained from comparing flame speeds with increment carbon chain agreed with Wang at al. [8] result stating that "the effect of the presence of ester group has a retarding effect on the overall mixture reactivity as the carbon chain increases". Also, good agreements were found between current results and few relevant esters studies of similar alkyl group or the same carbon numbers. A comparison between ester and alkane group has shown that the flame speed for both of them follows the same trend with carbon chain length. It is clear at low temperatures that the fuel with higher carbon chain has lower flame speed; however at high temperature the differences are negligible. In conclusion, the heat flux method is not a useful technique to study liquid fuels for high molecular mass, or in particular not able to determine the burning velocity of ester fuels of carbon chain length longer than C5 at current liquid heat flux installation.

Recommendations

Some recommendations can be considered to improve the experimental setup and to extend the ester fuels study in order to reach a high level of accurate results:

- The experiment could be extended with a higher temperature range, for this purpose the water bath have to be replaced with another heating medium which has a higher boiling point, for example oil bath. This includes the construction materials for burner head plate, plenum chamber and hoses… etc. which need to be adapted to higher temperatures.
- A heating tube could be used to keep the unburned mixture temperature at the same temperature while passing to the plenum chamber. This improvement could be extended the measurements to a high level of equivalence ratio and circumvent the partial pressure limitations. Therefore, combustion of more esters with higher molecular weights can be performed.
- Extend the same work with another fuel (ester group) or other type of fuel to compare it with the current results and draw clear conclusion.
- More research could be done with the same esters using another combustion method, for example, counter flow methods or closed vessel methods for comparing the results with heat flux method results for these esters. With the closed vessel method variable pressure and higher temperature could be obtained.
- The kinetic modelling could be performed for methyl acetate and ethyl acetate to compare it with experimental results to validate the accuracy of these models. A new kinetic modelling mechanism could be designed for n-propyl acetate.
- Different mixtures could be created from these esters and more experiments have to be performed to investigate the reliability of burning velocities and compare these results with burning velocities of purified esters. Also, mixtur results could be compared with theoretical flame speed prediction methods.

Many researches could be performed and a high level of accuracy could be obtained if the above recommendations were applied.

Bibliography

[1]   Øverland, I.; Kjærnet, H., Russian renewable energy: the potential for international cooperation, Farnham: Ashgate Publishing Company, 2009.

[2]   Schubert, R.; Schellnhuber, H.J.; Buchmann, N.; Epiney, A.; GrieBhammer, R.; Kulessa, M.; Messner,D.; Rahmstorf, S.; Schmid, J. , Future Bioenergy and Sustainable Land Use, London: Earthscan, 2010.

[3]   J. Buffam, K. Cox, H. Schiess, "Measurement of Laminar Burning Velocity of Methan-Air Mixtures Using a Slot and Bunsen Burner," WORCESTER POlYTECHNIC INSTITUE, 2008.

[4]   van Lipzig, J.P.J.; Nilsson, E. J. K.; de Goey, L.P.H.; Konnov,A.A., "Laminar burning velocities of n-heptane, iso-octane, ethanol and their binary and tertiary mixtures," *Fuel,* vol. 90, no. 8, pp. 2773-2781, 2011.

[5]   Seshadri, K., T.F. Lu, et al., "Experimental and kinetic modeling study of extinction and ignition of methyl decanoate in laminar non-premixed flows," *Proceedings of the Combustion Institute,* vol. 32, pp. 1067-1074, 2009.

[6]   Liu, W., Kelley, A.P., and law, C.K., "Non-premixed ignition laminar flame propagation, and mechanism reduction of n-butanol, and methyl butanoate," *Proceedings of the Combustion Insttitute,* vol. 33, pp. 995-1002, 2011.

[7]   Dooley, S., M.P. Burke, et al., "Methyl Formate Oxidation: Speciation Data, Laminar Burning Velocities, Ignition delay Times, and a Validated Chemical Kinetic Model," *International Jornal of Chemical Kinetics ,* vol. 42, no. 9, pp. 527-549, 2010.

[8]   Wang, Y.L., Q. Feng, et al., "Studies of C(4) and C(10) methyl ester flames," *Combustion and Flame,* vol. 158, no. 8, pp. 1507-1519, 2011.

[9]   Dayma,G. F. Foucher, et al., "Burning Velocities of C4-C7 Ethyl Esters in Spherical Combustion Chamber: Experimental and Detailed Kinetic Modeling," *Energy Fuels,* vol. 26, no. 11, pp. 6669-6677, 2012.

[10] "Chemical Book," 2008. [Online]. Available: http://www.chemicalbook.com/. [Accessed 7 11 2012].

[11] J. B. a. D. Spalding, "The laminar flame speed of propane/air mixtures with heat extraction from the flame," *Proc. Ror. Lond. A,* p. 255:71, 1954.

[12] L.P.H. de Goey, A. van Maaren and R.M. Quax, "Stabilization of adiabatic pemixd laminar flames on a flat-flame burner," *Cobust. Sci. Tech.,* vol. 92, pp. 201-207, 1993.

[13] A. v. Maaren, "One-step chemical reaction parmeters for premixed laminar flame," Eindhoven University of Technology, 1994.

[14] R. Meuwissen, "Extension of the heat flux method to liquid (bio-) fuel.," Eindhoven University of Technology, 2009.

[15] J. v. Lipzig, "Flame speed investigation of ethanol, n-heptane and iso-octane using the heat flux method," Lund University, 2010.

[16] K. Bosschaart, "Analysis of the heat flux method for measuring burning velocities," Eindhoven University of Technology, 2002.

[17] "Vädret i Sverige," [Online]. Available: http://www.smhi.se/vadret/. [Accessed Before taking measurements in any day].

[18] Vancoillie, J., Christensen, M., et al. , "Temperature Dependence of Laminar Burning Velocity of Methanol Flames," vol. 26, no. 3, pp. 1557-1564, 2011.

[19] Bosschaart, K.J., de Goey, L.P.H., "Detailed analysis of the heat flux method for measuring burning velocities," *Combustion and Flame,* vol. 132, pp. 170-180, 2003.

[20] L.P.H de Goey, L.M.T. Somers, W.M.M.L Bosch and R.M:M Mallens , "Modeling of the small scale structure of flat burner-stabilized flames," *Combust. Sci. and Tech.,* vol. 104, pp. 287-400, 1995.

[21] H. Boer, "Precision Mass Flow Metering For CVD Application.," Research Department of Bronkhorst High-Tech B.V., [Online]. Available: http://www.bronkhorst.com/files/published_articles/precision-mass-flow-metering.pdf. [Accessed 2012 10 21].

[22] Bios, "MesaLabs Bios," Bios International Corporation, 2009. [Online]. Available: http://www.biosint.com/pdf/Bios_Definer_Manual.pdf. [Accessed 25 11 2012].

[23] Ritter, Writer, *Accessories Thermometer Packing Liquid ,TG series Data Sheet and Drum-Type Gas Meters Operation Instructions.* [Performance]. LITREMETER Specialist Flow Measurement Engineering, 07/2010.

[24] Ritter, "Litremeter," Litremeter, Specialist Flow Measurement Engineering, [Online]. Available: http://www.litremeter.com/Technology/Gas_Meters.php. [Accessed 10 12 1012].

[25] I. manual, Writer, *General instruction digital Mass Flow/Pressure instruments laboratory style/IN-*

FLOW. [Performance]. Bronkhorst HIGH-TECH, 22-02-2010.

[26] Ranzi, E., Frassoldati, A., Grana, R., Cuoci, A., Faravelli, T., Kelley, A,P., Law, C.K., "Hierarchical and comparative kinetic modelling of laminar flame speeds of hydrocarbon and oxygenated fuels," *Progress in Energy and Combustion Science ,* vol. 38, pp. 468-501, 2012.

Appendix A

 Table of adiabatic burning velocities for three bio-fuel Esters at temperature range $298\,\text{k} - 348\,\text{K}$.

Burning Velocity for Methyl Acetate at temperature $T = 298\,K$		
Equivalence Ratio	Laminar Flame Velocity	Uncertainty
0.7	16.56	± 0.58
0.8	23.58	± 0.47
0.9	26.88	± 0.65
1	30.55	± 0.62
1.1	32.22	± 0.63
1.2	31.59	± 0.64
1.3	28.82	± 0.73
1.4	23.89	± 0.82
1.5	17.21	± 1.07
Burning Velocity for Methyl Acetate at temperature $T = 318\,K$		
Equivalence Ratio	Laminar Flame Velocity	Uncertainty
0.7	18.07	± 0.55
0.8	24.56	± 0.52
0.9	30.16	± 0.54
1	34.09	± 0.57
1.1	35.85	± 0.61
1.2	35.06	± 0.61
1.3	31.87	± 0.71
1.4	26.34	± 0.88
1.5	19.65	± 1.95
Burning Velocity for Methyl Acetate at temperature $T = 338\,K$		
Equivalence Ratio	Laminar Flame Velocity	Uncertainty
0.7	20.38	± 0.37
0.8	27.47	± 0.42
0.9	33.57	± 0.59
1	37.65	± 0.56
1.1	39.57	± 0.60

1.2	38.75	± 0.61
1.3	35.46	± 0.69
1.4	30.63	± 1.57

Burning Velocity for Methyl Acetate at temperature $T = 348\ K$		
Equivalence Ratio	Laminar Flame Velocity	Uncertainty
0.7	22.39	±4.18
0.8	29.35	±3.22
0.9	35.30	±2.84
1.0	39.21	±2.93
1.1	41.20	±3.28
1.2	38.88	±2.39
1.3	35.13	±3.29
1.4	29.35	±7.65

Note: measurements at $T = 348\ K$ taken under different thermocouple connection

Burning Velocity for Ethyl Acetate at temperature $T = 298\ K$		
Equivalence Ratio	Laminar Flame Velocity	Uncertainty
0.7	17.30	± 0.83
0.8	23.24	± 0.57
0.9	28.28	± 0.70
1	31.38	± 0.66
1.1	32.09	± 0.65
1.2	30.12	± 0.69
1.3	25.68	± 0.84
Burning Velocity for Ethyl Acetate at temperature $T = 318\ K$		
Equivalence Ratio	Laminar Flame Velocity	Uncertainty
0.7	19.53	± 0.50
0.8	26.12	± 0.55
0.9	31.37	± 0.59
1	34.72	± 0.58
1.1	35.41	± 0.59
1.2	33.38	± 0.65
1.3	28.74	± 0.73
Burning Velocity for Ethyl Acetate at temperature $T = 338\ K$		
Equivalence Ratio	Laminar Flame Velocity	Uncertainty
0.7	22.02	± 0.41
0.8	29.02	± 0.44
0.9	34.83	± 0.50
1	38.25	± 0.48
1.1	39.07	± 0.58
Burning Velocity for Ethyl Acetate at temperature $T = 348\ K$		
Equivalence Ratio	Laminar Flame Velocity	Uncertainty
0.7	23.40	± 0.35
0.8	30.76	± 0.36
0.9	36.77	± 0.55

| 1.0 | 40.70 | ± 0.62 |
| 1.1 | 41.14 | ± 0.62 |

Burning Velocity for n-Propyl Acetate at temperature T=298K		
Equivalence Ratio	Laminar Flame Velocity	Uncertainty
0.7	16.25	± 0.62
0.8	22.05	± 0.77
0.9	27.08	± 0.73
1	29.93	± 0.71
1.1	30.29	± 0.66
1.2	28.04	± 0.67
Burning Velocity for n-propyl Acetate at temperature $T = 318\,K$		
Equivalence Ratio	Laminar Flame Velocity	Uncertainty
0.7	18.58	± 0.58
0.8	25.13	± 0.59
0.9	30.20	± 0.55
1	33.27	± 0.57
1.1	33.57	± 0.59
1.2	31.04	± 0.68
Burning Velocity for n-Propyl Acetate at temperature $T = 338\,K$		
Equivalence Ratio	Laminar Flame Velocity	Uncertainty
0.7	21.16	± 0.36
0.8	28.12	± 0.41
0.9	33.55	± 0.49
1.0	36.79	± 0.52
1.1	37.12	± 0.58
Burning Velocity for n-Propyl Acetate at temperature $T = 348\,K$		
Equivalence Ratio	Laminar Flame Velocity	Uncertainty
0.7	23.67	
0.8	30.55	
0.9	36.31	
1.0	39.31	
1.1	40.06	

Note: measurements at $T = 348\,K$ taken under different thermocouple connection